Optimizing soft-switching operation of GaN at high frequency

About this document

Scope and purpose

The document is structured into two chapters. In Chapter 1, an overview and positioning of the three different semiconductor technologies (Si, SiC, GaN) is provided. Chapter 2 presents examples of topologies suitable for soft switching high-frequency operation, focusing on key applications in switch mode power conversion.

Intended audience

The primary audience for this white paper includes R&D Design Managers and Engineers with a solid background in Switch Mode Power Supply (SMPS) design. Therefore, some basic concepts on power conversion topologies are assumed to be known.

Moreover, Product Qualification Engineers and Procurement Managers at SMPS companies will also find valuable information relevant to their roles here.

Key points

Extensive technical literature suggests that GaN is the ideal power device for high-frequency power conversion. This document provides an in-depth analysis of the key features that make GaN technology attractive and highly efficient at high switching frequencies, up to the ~1 MHz range.

About this product family

Product family

Infineon's CoolGaN™ product family offers a range of power transistors offering a versatile and scalable solution for consumer and industrial applications. With a broad voltage range of 60 V to 700 V and various packages, they offer superior switching speed, high-power density, and reduced energy losses, resulting in smaller, lighter, and more compact systems with improved reliability and thermal conductivity. With their higher thermal conductivity and robust design, they are capable of withstanding high-voltage spikes and ensuring a longer lifespan, making them an ideal choice for designers seeking to create innovative and efficient power management solutions.

Target applications

- Powering AI PSU solutions
- Telecommunications infrastructure
- Adapters and chargers
- Microinverter solutions

Table of contents

1 Positioning and perspective of GaN-based power devices

After the recent market introduction of GaN-based power devices, there are now three major technologies, i.e., silicon superjunction, silicon carbide, and gallium nitride, with various device concepts competing in the 600 V/650 V class. This chapter will briefly introduce the key characteristics of the different technologies and provide a positioning of the technologies in different applications.

1.1 Technology of GaN HEMTs

GaN-based power devices can be classified into vertical and lateral concepts, as well as normally-on and normally-off devices. Vertical devices have limitations due to the cost and availability of bulk GaN substrates, which pose a major hurdle for their development. Furthermore, vertical JFET structures forming either normally-on or normally-off channels are also available in SiC, which reduces the value proposition of vertical GaN devices.

Lateral devices, on the other hand, feature high electron mobility and create a natural two-dimensional electron gas (2DEG) at the interface of GaN and AlGaN layers. This characteristic creates advantages in the figure-of-merit $R_{DS(on)} \times Q_{oss}$, as less electrons are needed for a given load current.

The formation of the 2DEG leads naturally to normally-on devices. On the one hand, these can be turned into normally-off circuits by adding a low-voltage MOSFET in series with the normally-on device. The circuit can be either controlled in a cascode mode by turning on/off the LV MOSFET or in direct-drive mode by controlling the normally-on device directly while keeping the LV MOSFET always on. The latter method allows good control of switching characteristics with respect to dv/dt and di/dt, while the cascode arrangement suffers from lack of feedback capacitance from the normally-on device into the driving circuit.

On the other hand, the GaN device itself can also be turned into a normally-off device either with the Schottky gate or the gate-injection transistor concept. The gate-injection concept is more forgiving towards imperfect layouts as the p-GaN gate naturally clamps any overvoltage to the threshold of its forward-biased diode characteristic. By controlling this forward current into the gate, the effective gate voltage can be well controlled independently on the voltage drop across the source-to-gate region. The injection of holes from the p-GaN gate further enhances the concentration of electrons in the 2DEG and creates an advantageous conductivity modulation effect.

In the following sections, we refer to GaN-on-Silicon devices prevailing today in the 600 V–650 V class. Device concepts based on GaN-on-Sapphire or GaN on engineered substrates such as QST are typically targeting the 1200 V range.

Detailed information on operation descriptions, recommendations and guidelines on layout, and gate driving of GaN HEMTs are provided in [1], [2], and [3].

1.2 Technology of silicon superjunction and silicon carbide

GaN HEMTs compete with silicon superjunction devices and SiC MOSFETs in many applications. Figure 1 compares the key figure-of-merits of SiC MOSFETs and GaN HEMTs with the established CoolMOS™ C7 Superjunction technology. The superjunction concept will continue to improve, with the upcoming CoolMOS™ C8 technology offering an $R_{DS(on)}$ as low as 16 mΩ in a standard TO220 package. This significant reduction in on-state resistance will further reduce conduction losses and increase the overall efficiency of power conversion systems [4].

Device	$V_{(BR)DSS}$ [V]	$R_{DS(on)}*E_{oss}$	$R_{DS(on)}*Q_g$	$R_{DS(on)}*Q_{oss}$	$R_{DS(on)}*Q_{rr}$
CoolMOS™	600	100%	100%	100%	100%
CoolGaN™	650	79%	11%	9%	0%
CoolSiC™	650	83%	39%	11%	2%

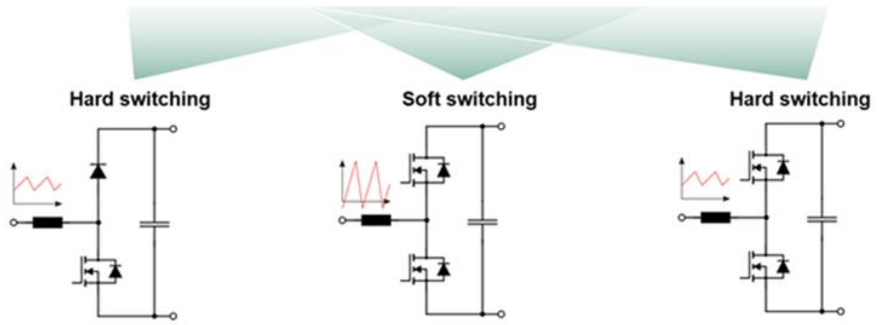

Figure 1 Comparison of key figure-of-merits of the Si, GaN, and SiC technologies' latest generations and their relevance for fundamental switching operation

In the field of SiC devices, normally-on vertical JFET structures and normally-off MOSFETs (either with planar or vertical gate structures) co-exist on the market. MOSFETs have a relatively low increase of $R_{DS(on)}$ with temperature, making them suitable for high-temperature applications. This is particularly important in applications where the device is subjected to high ambient temperatures or high-power densities. Vertical gate structures offer natural protection of the gate oxide in the blocking state without compromising on-state resistance, making them a preferred concept for many applications.

1.3 Positioning of technologies

In half-bridge circuits, hard-switching losses are dominated by the FoMs $R_{DS(on)} \times Q_{oss}$ and $R_{DS(on)} \times Q_{rr}$. SiC MOSFETs have significantly reduced reverse recovery charge, whereas GaN-based HEMTs feature zero reverse recovery charge. In addition, both wide bandgap devices have a massively reduced output charge Q_{oss} by almost an order of magnitude [5]. Therefore, both GaN HEMTs and SiC MOSFETs enable continuous hard-switching operation of half-bridges, which is not possible with Si superjunction devices.

Of all device concepts, GaN-based HEMTs exhibit the lowest gate charge and are therefore the best choice in the very-high switching frequency domain such as power conversion beyond 400 kHz–500 kHz. In this frequency domain, soft switching with zero voltage turn-on is the only choice, as hard switching would lead to excessive losses. The combination of rapid turn-off transitions and the elimination of E_{oss}-associated losses through the ZVS transition enables the achievement of excellent efficiency and power density [6]. It is crucial to note that a fast turn-off with zero losses requires the load current to be turned off through the channel at or before the point in time when the device begins to block voltage. GaN HEMTs, with their unique combination of low gate charge, steep transconductance, and low driving voltage, are well suited to achieve this.

In summary, silicon superjunction devices demonstrate superior performance in single-ended hard-switching applications and resonant converters operating at low to moderate switching frequencies. On the other hand, SiC devices offer significant advantages in hard-switching half-bridge and full-bridge circuits. Meanwhile, GaN HEMTs showcase their exceptional capabilities in the high-frequency domain, particularly in resonant converters, and in topologies that employ triangular current modulation.

2 GaN application in high switching frequency topologies

2.1 Resonant LLC

The LLC resonant converter is a typical example of a soft-switching topology, which has increased in popularity in recent years thanks to its promise to provide highly efficient, compact, and isolated power conversion for numerous applications. In a nutshell, the advantages of the LLC resonant converter are that all primary devices can achieve zero voltage switching (ZVS) during the entire load range, and the secondary-side synchronous rectification (SR) devices can also achieve zero current switching (ZCS) when the converter operates at or below the resonance. These benefits make the LLC resonant converter inherently suitable for highly efficient operation at high switching frequency. The following paragraphs explain how the HV and MV GaN device properties provide unique benefits to the LLC operation, by minimizing power losses both directly (on the devices themselves) and indirectly (e.g., on the main transformer).

2.1.1 Value proposition of GaN in resonant LLC

Figure 2 shows the well-known principle schematic of an HB LLC. This topology will be used as the main reference to explain the general benefits of GaN in resonant power converters operating at high switching frequency.

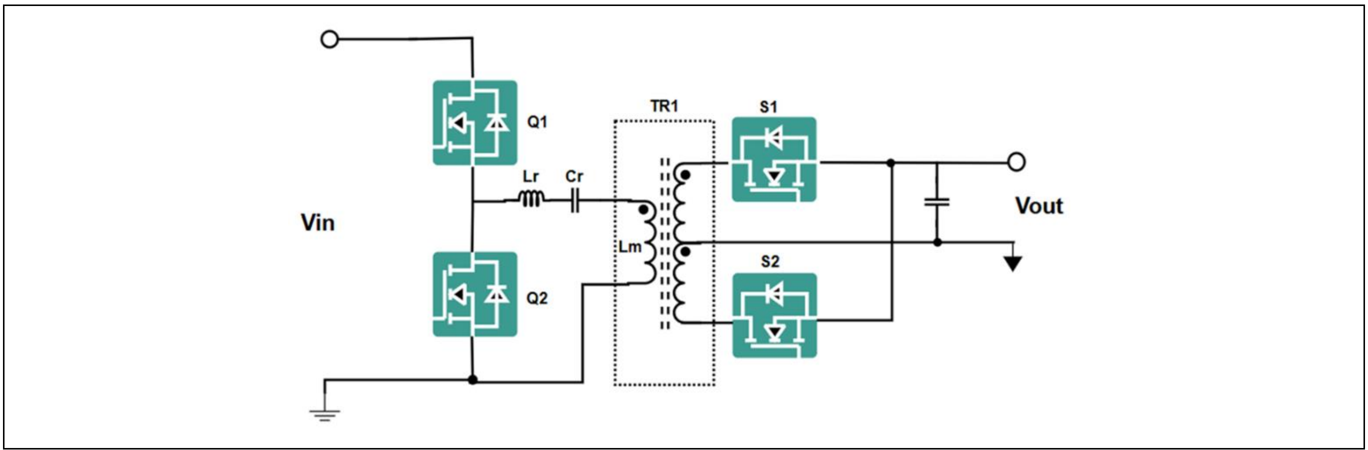

Figure 2 Principle schematics of a HB LLC

2.1.1.1 HV GaN on the primary side of a HB LLC

The LLC resonant converter operating at the resonance realizes high efficiency at high frequency due to the soft-switching of both primary side and secondary side devices. Figure 3 shows the typical waveforms on the primary side of an LLC converter switching at its resonance frequency.

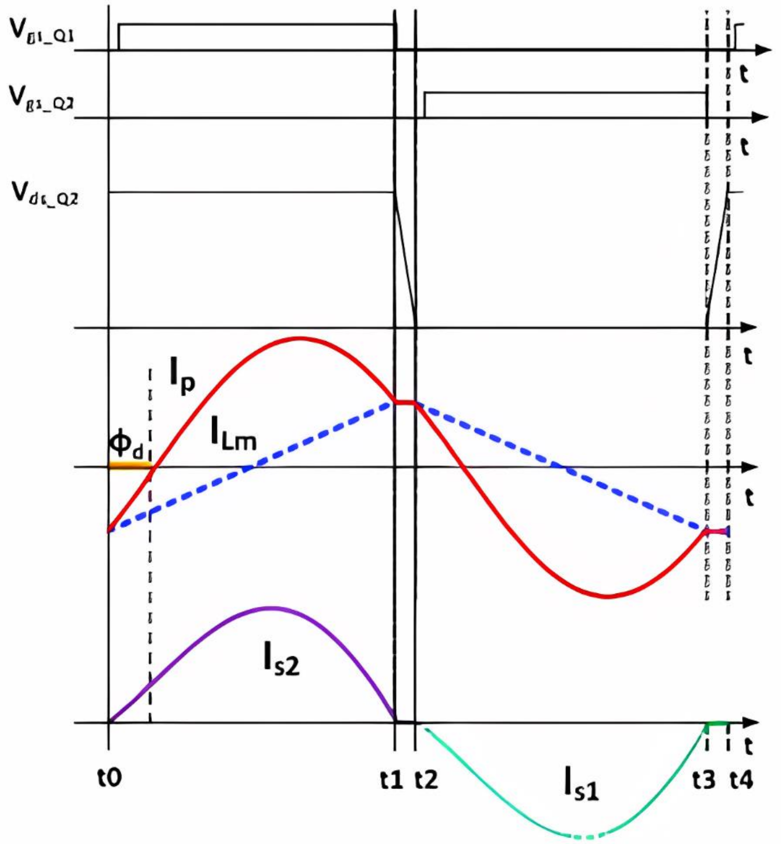

Figure 3 Waveforms of the HB LLC Converter running at the resonance frequency

During the dead-time (t1–t2), the drain-source voltage of Q2 drops to zero by the magnetizing current I_{Lm} discharging the device output capacitances. Q2 then turns on with ZVS. In order to guarantee ZVS of the devices, sufficient peak magnetizing current and dead-time are needed to ensure that all the parasitic capacitances have been discharged, including the output capacitances of the primary-side and secondary-side devices, as well as the transformer winding capacitances. During the dead-time (t1–t2), the magnetizing current can be approximated as a current source ($I_{m,pk}$). For the primary-side half-bridge topology, the device ZVS can be described by the following equation, which links the minimum dead-time setting to the device Q_{oss} (at DC_bus voltage = 400 V) and the peak magnetizing current.

$$t_{dead,min} = 2 \cdot \frac{\mathrm{Qoss@400\ V}}{\mathrm{Im,pk}}$$

Equation 1 Equation to calculate the minimum dead-time for device ZVS

The key implications of this relationship are quickly summarized in Figure 4.

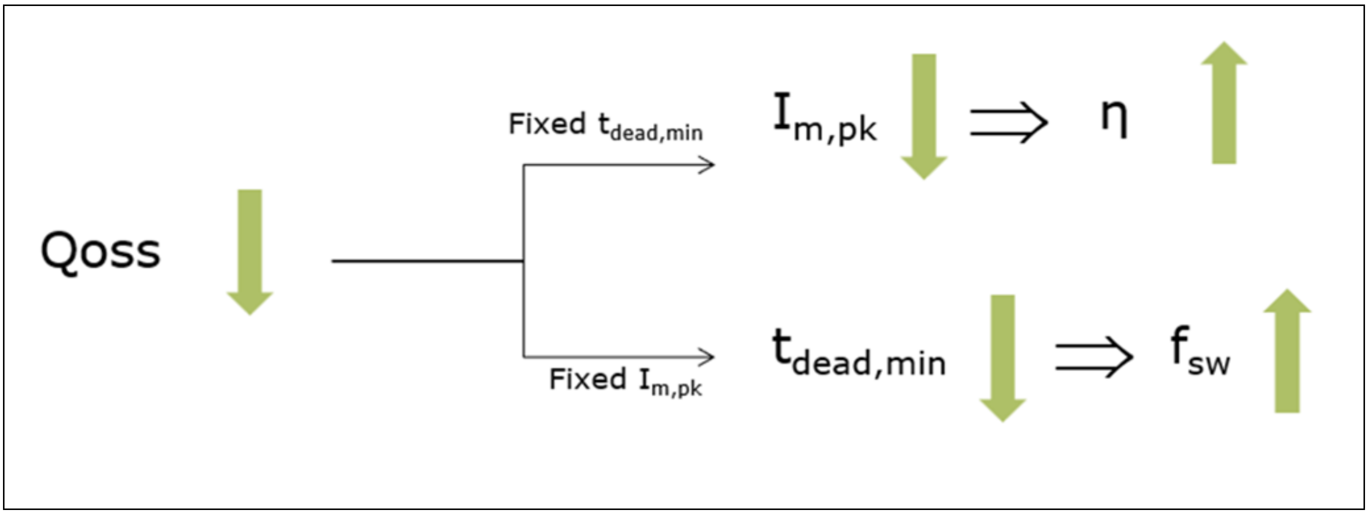

Figure 4 Benefits of HV devices with low Q_{oss} in HB LLC

In other words, the benefits of using HV devices with low Q_{oss} on the primary side are in two directions, based on the main design scope. If efficiency is the main focus, for a fixed minimum dead-time setting, the peak magnetizing current can be minimized, with less conduction losses on both primary devices and transformer windings.

On the contrary, if high switching frequency is the main target of the HB LLC design, for a given peak magnetizing current, the low Q_{oss} of the HV devices enables the reduction of the minimum dead-time setting necessary to get ZVS operation.

Let us try to understand the benefits of GaN with respect to Q_{oss}. Figure 5 shows a direct comparison of the FOM $R_{DS(on)} \times Q_{oss}$ of the latest generations of all three technologies. From the image, it is clear that GaN has the lowest FOM, thus making it the best one.

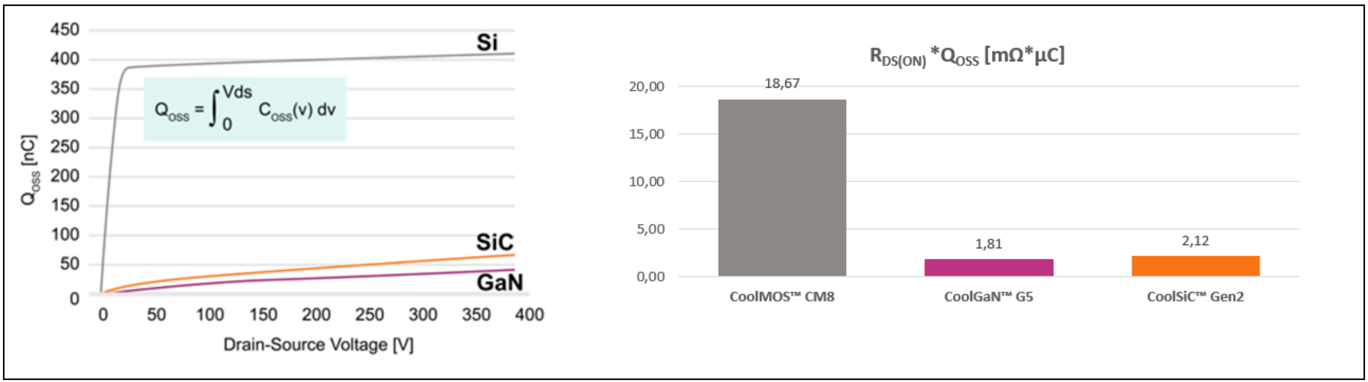

Figure 5 Q_{oss} vs. V_{DS} and $R_{DS(on)} \times Q_{OSS}$ comparison of the latest generations of HV Si, SiC, and GaN technologies (T_j = 25°C)

Looking from a different perspective, Figure 6 shows that a longer dead-time leads to a higher primary RMS current, and thus higher conduction losses.

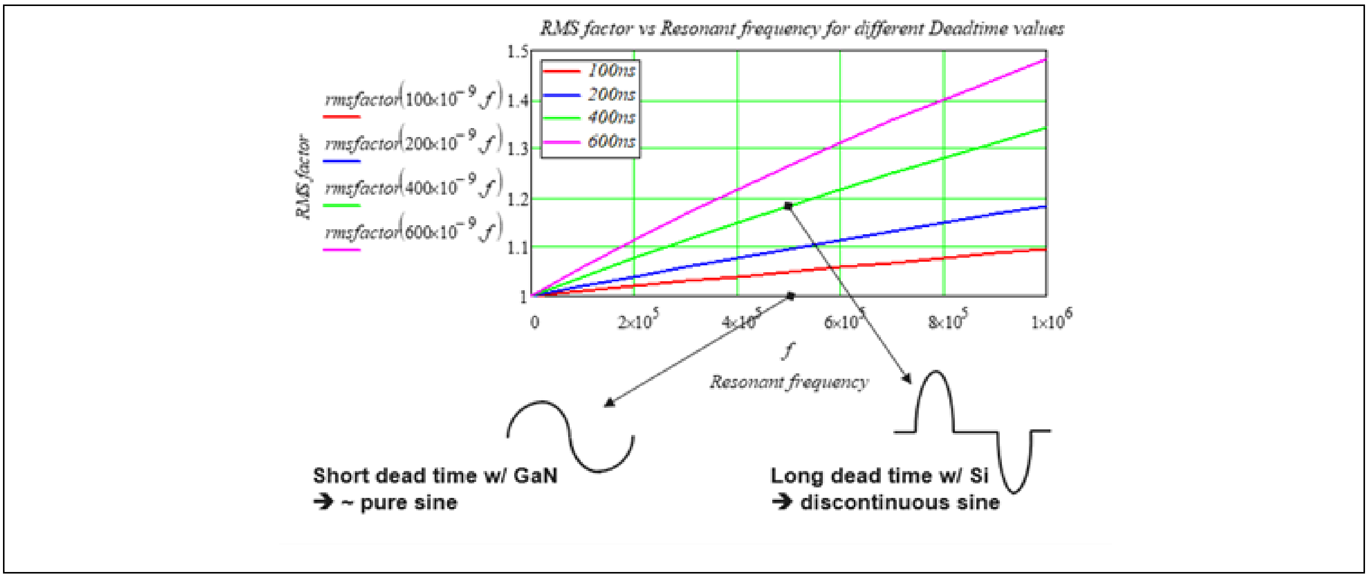

Figure 6 Primary RMS current vs. resonant frequency for different dead-time values

Technical literature [7] demonstrates that, in general, the power device loss in LLC converter (P_{tot}) can be expressed as a function of dead-time (T_d) and the transformer's winding capacitance (C_w). There is always a minimum loss point at a certain dead-time point and winding capacitance, as shown in Figure 7. It is possible to demonstrate that, mainly due to the lowest Q_{oss}, GaN devices are the best fit for LLC transformers with a construction that helps minimize winding losses, despite an increase of the winding capacitance. An example of such transformers is given by the planar transformers, largely used in the compact form factor LLC converters of high-power density SMPS. Therefore, this is another reason why GaN devices are beneficial in high power density designs.

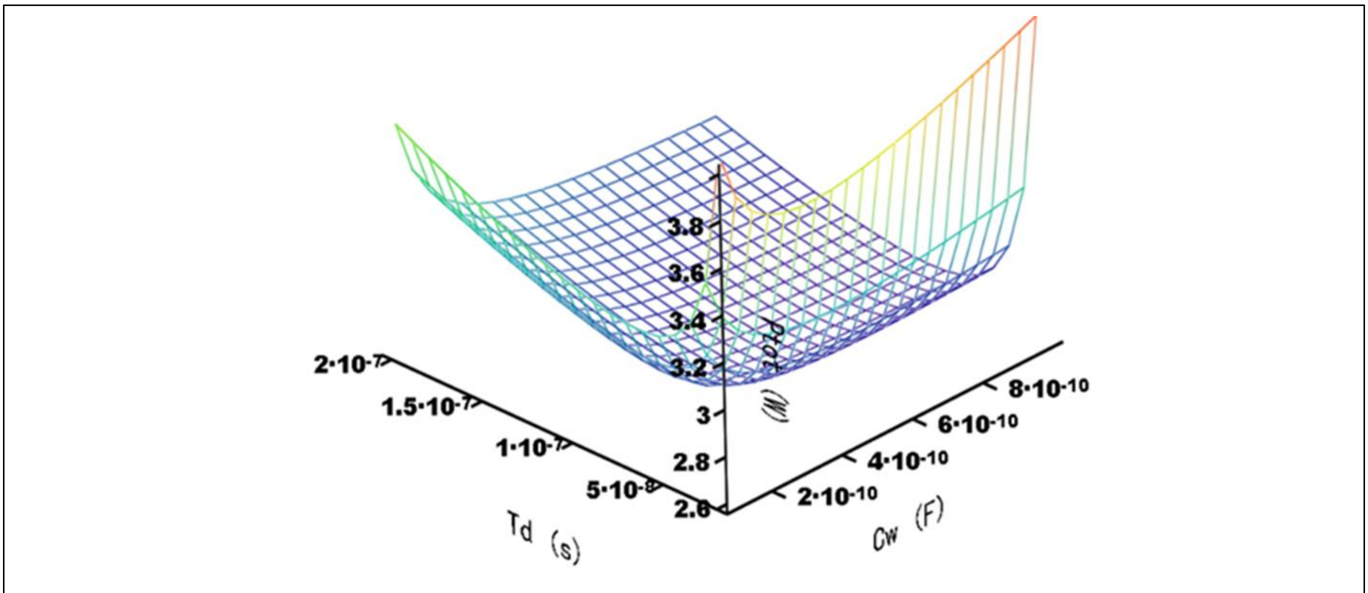

Figure 7 Total device loss vs. dead-time and winding capacitance

Another relevant loss mechanism significantly affecting the efficiency at mid to heavy load operation of LLC topologies occurs at the turn-off. In fact, whilst the ZVS is achieved at turn-on, losses occur at the turn-off, where certain current and voltage overlap is possible.

GaN application in high switching frequency topologies

The lowest Q_g and Q_{gd} parameters among the HV technologies inherently give the GaN the lowest FOM (E_{OFF}), as highlighted in Figure 8.

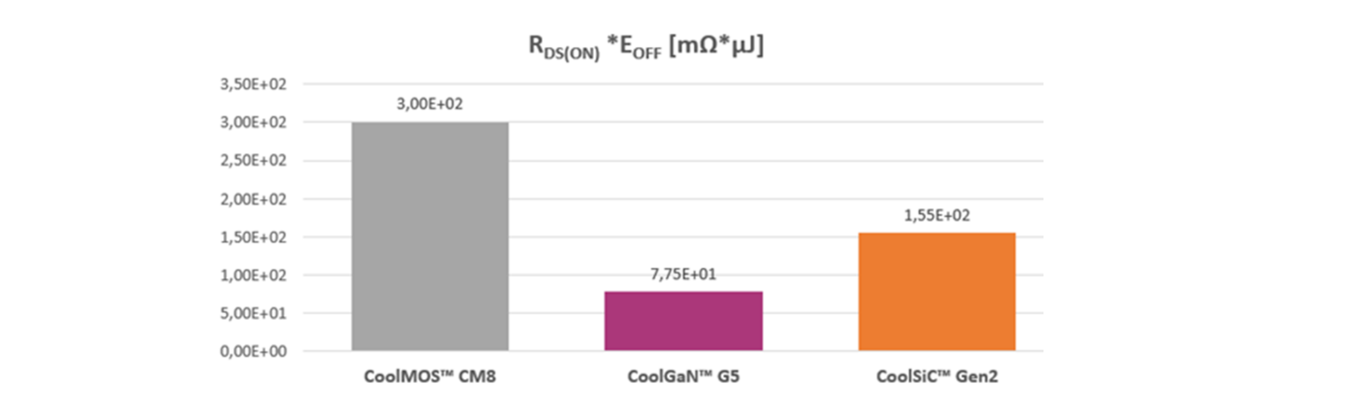

Figure 8 $R_{DS(on)} \times E_{OFF}$ **comparison of the latest generations of HV Si, SiC, and GaN technologies (T_j = 25°C)**

2.1.1.1 MV GaN in the synchronous rectification stage on the secondary side of an HB LLC

So far, MOSFETs have typically been observed on the secondary side as synchronous rectifiers (SRs) for LLC converters, despite their higher Q_g-related losses compared to GaN. On the other hand, the high output capacitance (C_{oss}) of the secondary switch increases the equivalent capacitance of the primary switching node just like transformer parasitic (interwinding) capacitance, necessitating a higher peak magnetizing current (i_{Lm}) for ZVS. This increases the RMS current on the primary-side due to increased circulation. Similarly, at no-load or very-light-load conditions, the LLC tank-gain behavior changes due to the high-frequency secondary-resonance. This is because the SR C_{oss} and the transformer parasitics change the load characteristics from resistive to capacitive, especially at no-load. For this purpose, Figure 9 shows the different primary current waveforms at no-load operation in case of legacy diode rectification vs. GaN SR vs. Si SR. Such a change results in an unexpected increase of the LLC tank-gain as the frequency increases, making no-load regulation challenging by putting a limit to the maximum switching frequency and/or requiring a dummy load to be employed as the minimum load.

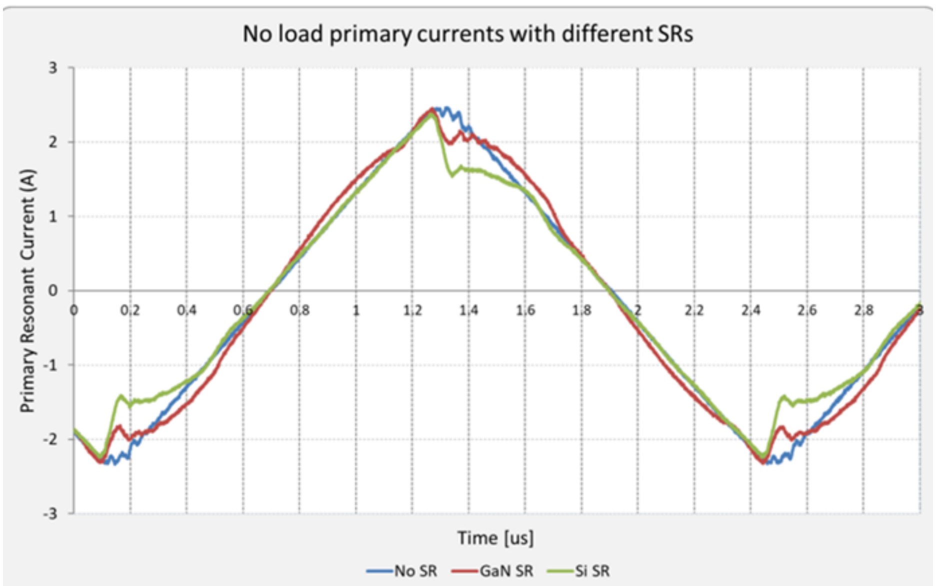

Figure 9 **No load primary currents with different SRs**

Transformer-magnetizing energy is employed for the ZVS condition of the primary switches in the LLC converter. This energy is proportional to the square of the peak magnetizing current as well as the transformer-magnetizing inductance value itself. The peak magnetizing inductance energy should be greater than the equivalent capacitive energy at the primary switching point to remove all the capacitive charge at all operating points. It can easily be concluded that the worst case for the available magnetizing energy for a certain LLC tank design occurs when the converter operates at the maximum switching frequency, which reduces the magnetizing current to its minimum.

The equivalent primary switching point capacitance is a combination of:

- Equivalent primary-switch C_{oss} transformer interwinding capacitance referred to the primary-side
- Layout-related parasitic capacitance
- Equivalent secondary-switch C_{oss} reflected to the primary-side
- Equivalent secondary-switch Q_{rr} reflected to the primary-side in above-resonance operation (MOSFET SR)

The above-resonance operation of the LLC converter results in an additional charge (Q_{rr}) to be removed on the secondary side in the case of the MOSFET SR, which makes the SR charge contribution equal to Q_{oss}+Q_{rr}. This additional energy as well as the SR device reverse-recovery loss is not observed in the case of GaN SR. Any increase in any of these capacitances will necessitate a higher ZVS energy as can be observed in Figure 10 where the silicon (Si) SR drains more magnetizing current compared to GaN. This can be obtained by lowering the transformer magnetizing inductance to increase the peak magnetizing current, which in turn increases the circulating current losses on the primary-side. GaN, having a lower device capacitance both on the primary-side and the secondary-side, is a high-efficiency enabler from this perspective. In addition, the lower magnetizing energy requirement implies a higher magnetizing inductance, resulting in a lower air gap for the same number of turns. This results in a lower fringing flux, which is a significant contributor to the transformer winding AC resistance value.

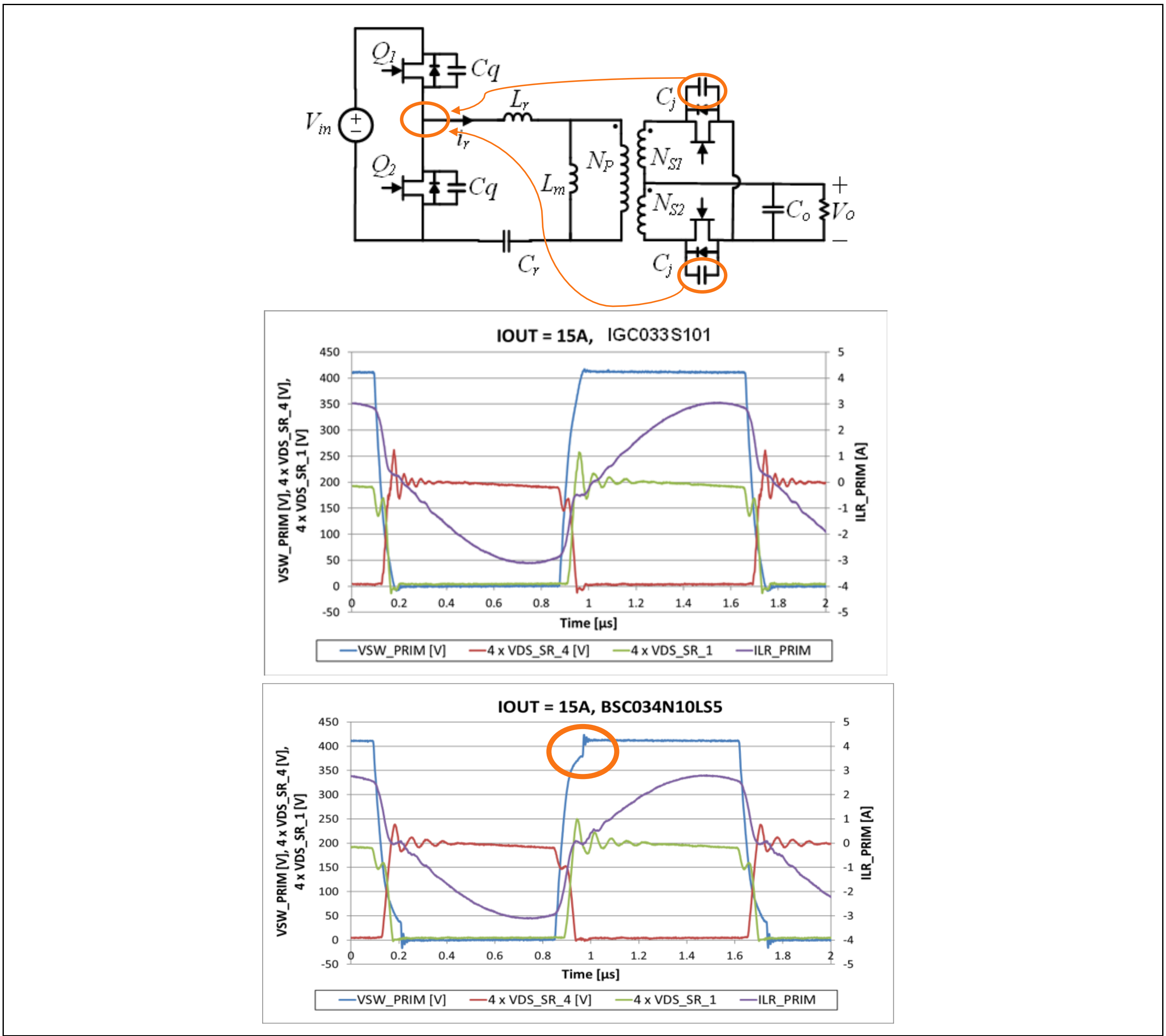

Figure 10 Typical primary and secondary waveforms in LLC topology: effect of SR devices output capacitance (MV Si vs. MV GaN)

No-load regulation is one of the challenges in LLC converter design. Here, the equivalent no-load impedance reflected to the primary-side comes in parallel to the magnetizing inductance (L_m). This impedance at no-load is mainly capacitive due to the parasitics, which results in an additional high-frequency resonance to be observed in the LLC converter gain-curve. So, the LLC tank-gain increases in high frequencies well above the resonance frequency during no-load conditions, which is contradictory to the LLC converter-control rule, which requires reduction of the output voltage with an increase of the switching frequency. To avoid this, it is a common practice to employ a dummy load with a maximum frequency limit so that the no-load operating point is kept away from this region.

Apart from a careful transformer and PCB layout design to minimize the parasitic capacitances, additional improvement comes from employing GaN switches on the secondary side as SRs as shown in Figure 11Figure 3. The lower device-capacitance of GaN pushes this additional resonance to even higher frequencies at no-load, which reduces the additional dummy-load requirement for stability. In addition, the high third-quadrant performance of the GaN device could be an advantage for no-load conditions since it is a common practice to completely turn off the SR switches to improve the no-load performance of the converters. This way, the tendency of the output voltage to increase due to the parasitic capacitances around the secondary resonance can be compensated by the third-quadrant voltage drop of a GaN SR.

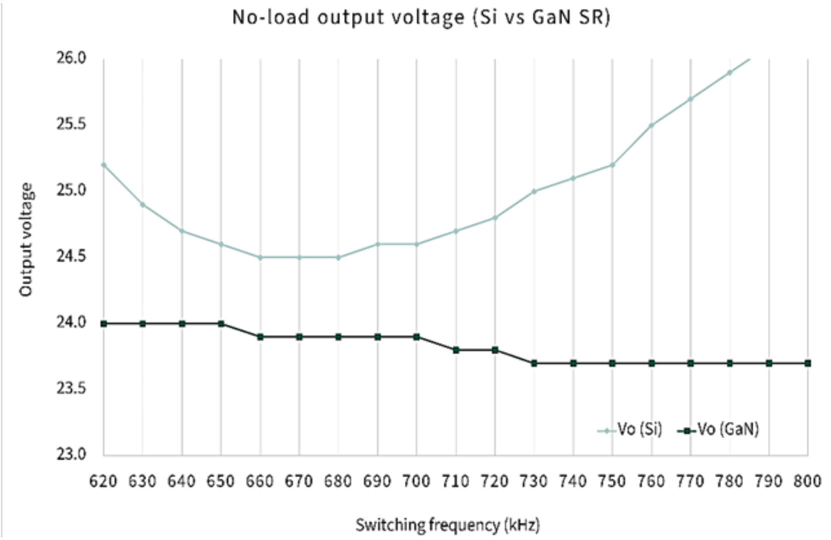

Figure 11 No-load output voltage (Si vs. GaN SR)

2.1.1.2 Effect of high switching frequency on dynamic and high-power transients

Aside from the significantly increasing power trend of the AI PSU, the GPU draws a higher peak power and generates high load transients, as shown in Figure 12. Therefore, the DC-DC stage output must be dynamic enough while the voltage overshoot and undershoot must stay within the specified limits. The DC-DC stage output dynamics can be increased by raising the switching frequency, thereby increasing the control loop bandwidth.

CoolGaN™ devices easily address this requirement of a higher switching frequency due to their superior FoM and the lowest switching losses among Si, SiC, and GaN devices. Especially in soft-switching LLC converters, CoolGaN™ has the lowest output capacitor charge (Q_{oss}), which plays a vital role in reaching ZVS more easily. Subsequently, this facilitates a more precise dead-time setting and thus eliminates unnecessary dead-time conduction losses.

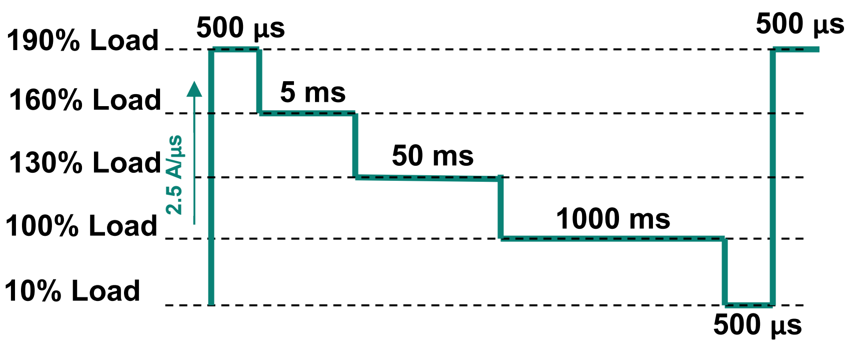

Figure 12 AI PSU peak power demanded by AI GPUs

2.1.2 Application example

As an application example, the HB LLC stage of the Infineon Technologies REF_3K3W_HFHD_PSU will be used as an optimal use case of GaN in a resonant topology. See [8] for a full description of the reference design. This design addresses a high-power density PSU for modern server and telecom applications.

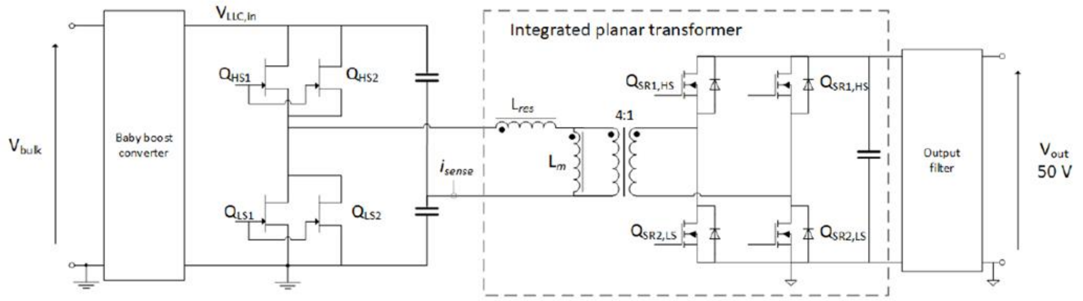

Figure 13 Simplified schematics of the HB LLC in REF_3K3W_HFHD_PSU

The selected resonant frequency is 530 kHz and the whole range of switching frequency is 450 kHz–1.5 MHz, and HV CoolGaN™ has been chosen for the converter's primary side, more precisely IGT65R035D2, 650 V, 35 mΩ $R_{DS(on)\_typ}$. The primary side of the LLC converter uses four of these devices, each having 35 mΩ $R_{DS(on)\_typ@Tj=25°C}$, in a TOLL package, with both high and low sides having two devices in parallel.

All the four GaN power switches and the related driving circuits have been placed on a daughter card, as typically done in modern modular SMPS design. The secondary SR MOSFETs are directly soldered on the secondary turns of the main planar transformers. Figure 14 shows the power daughter card and the planar transformer structure with integrated synchronous rectification stage.

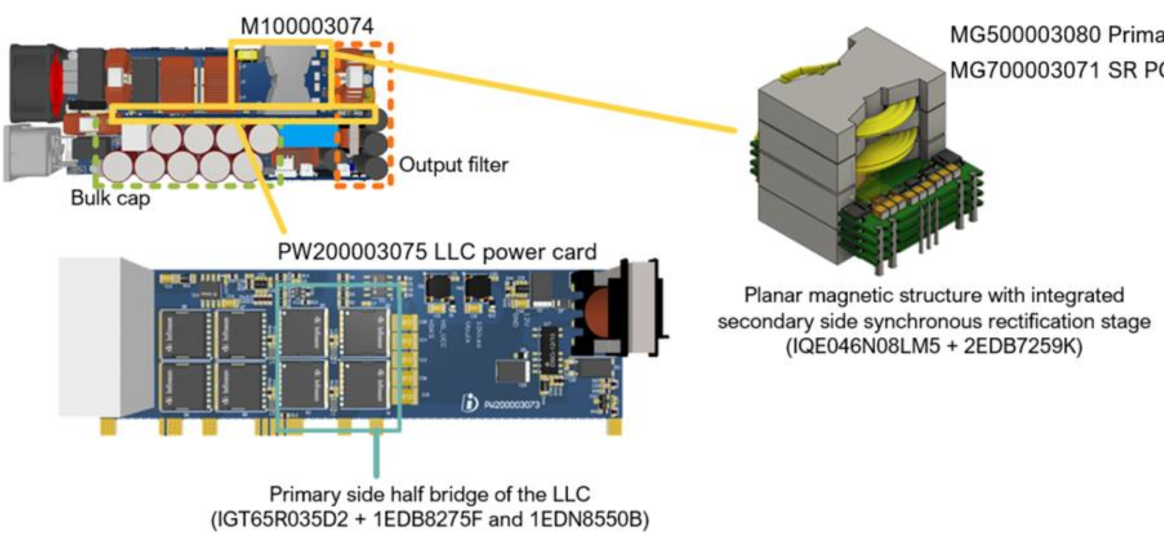

Figure 14 Primary and secondary sides of the HB LLC converter in the REF_3K3W_HFHD_PSU

This application example also gives us the opportunity to study the best way to design the transformer of an LLC converter operating at high switching frequency, as mentioned above, in the range of 450 kHz–1.5 MHz.

GaN application in high switching frequency topologies

In general, one of the advantages of the LLC topology is reusing the leakage inductance of the main transformer as the resonant inductance of the tank and the magnetizing inductance of the transformer as a parallel resonant inductor. Whilst this simplifies the resonant tank design, on the other hand this compromises the overall efficiency. To get an optimized efficiency in this design, series and parallel inductors have been integrated in the main transformer structure to minimize space.

Figure 15 shows the cross-section of the transformer structure. It is important to mention that the magnetic structure presented there is key to this design to achieve the LLC's target efficiency of 98.5%, the integration of the synchronous rectification stage, and the required power density.

Additional construction details of the main transformer are shown in Figure 16. The transformer has a turns ratio of 8:2 and its "stack" uses four primary and four secondary PCBs with full interleaving to reduce high-frequency copper losses. In between each PCB couple, an FR4 spacer is also inserted to increase the air gap between the windings, thus reducing the interwinding capacitance for each interleaving layer, and keeping it constant. It has been measured that the ring spacers between PCBs decrease the interwinding capacitance from about 140 pF (no spacers) to about 60 pF (with FR4 spacers).

Figure 16 also shows details of the MOSFET SRs (Infineon OptiMOS™ IQE046N08LM5) integrated in the secondary PCB turns, together with the respective gate drivers.

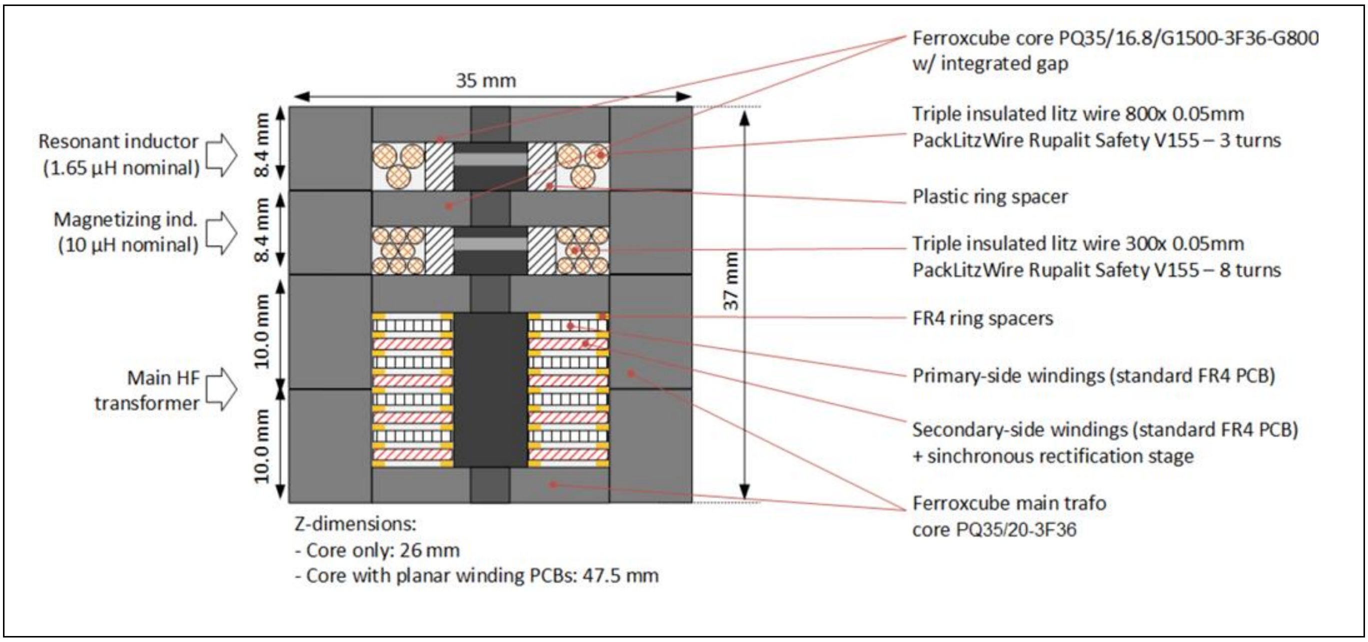

Figure 15 Integrated planar transformer cross section

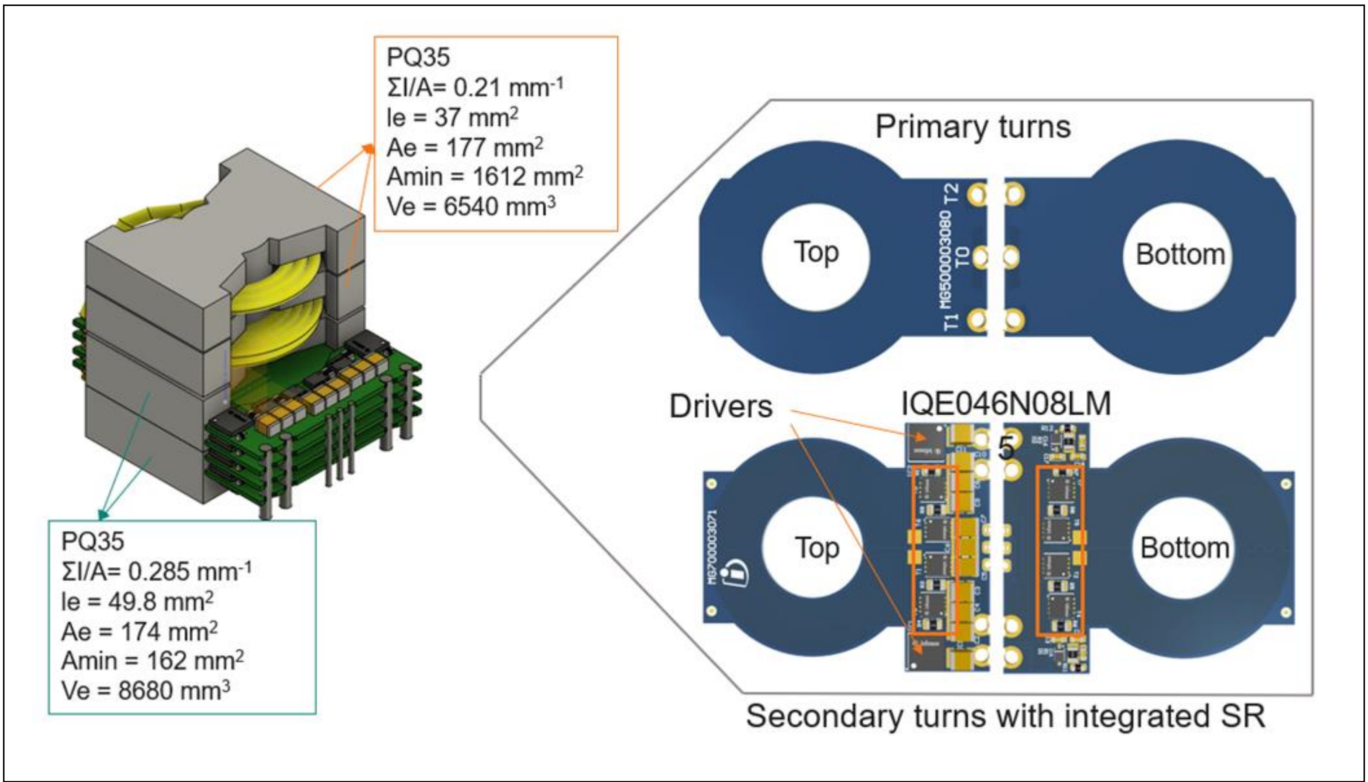

Figure 16 Transformer mechanical assembly stack

In Figure 17, the solid line shows the efficiency plot of the HB LLC converter at the nominal input voltage V_{in} = 400 V DC. It should be noted that the efficiency is ~98.5% at 50% of the rated load and remains around 98% at full-load. The dashed line in the same figure provides the converter losses at the same nominal input voltage V_{in} = 400 V DC.

It is also interesting to observe, in Figure 18, the estimation of the corresponding power losses breakdown. It can be seen that the main contributors to the power losses are conduction losses of the primary-side, the synchronous rectifiers, and total copper losses of the series and parallel inductance, and of the main transformer itself.

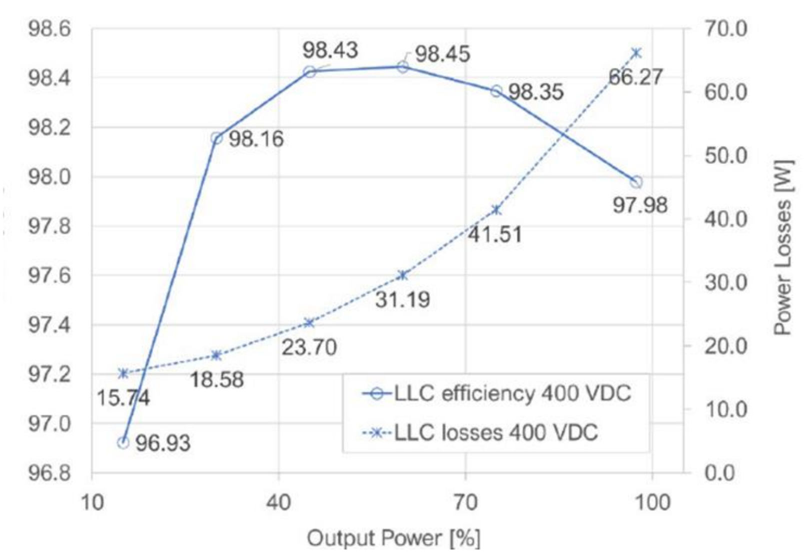

Figure 17 Efficiency of the HB LLC stage with a CoolGaN™ device having a 35 mΩ on-resistance

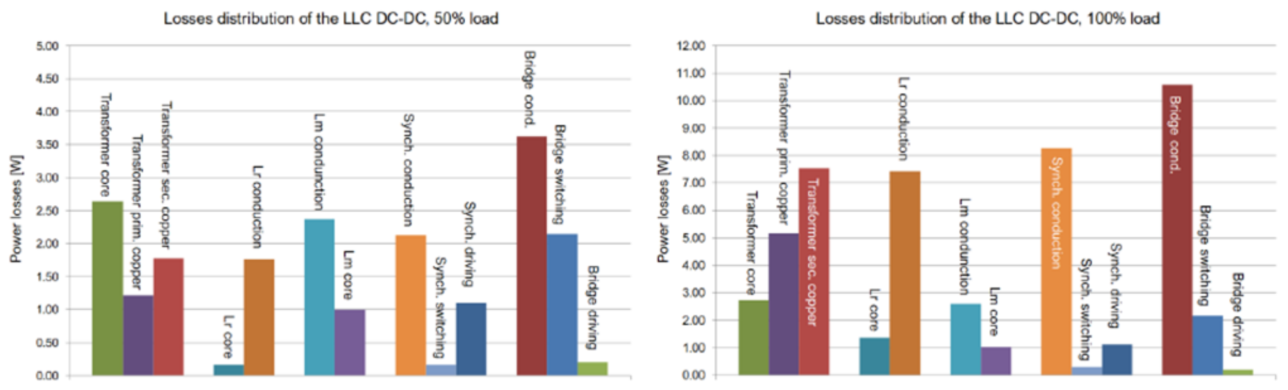

Figure 18 Power loss breakdown of the 3.3 kW HB LLC

Finally, Figure 19 and Figure 20 include the waveforms captured for the HB LLC primary and secondary sides during normal operation at 50% and 100% load. From the oscilloscope plots, it can be observed that full ZVS turn-on is achieved on the GaN devices at the primary side primary in both conditions, along with a lossless turn-off.

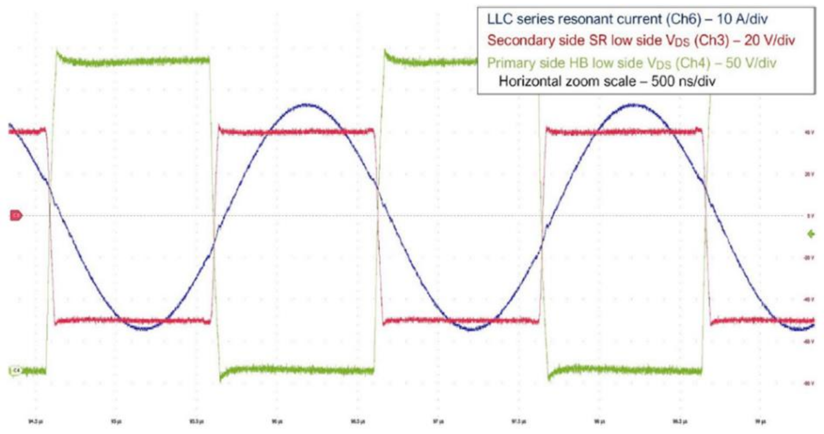

Figure 19 LLC waveforms during steady-state operation at 50% of the rated load

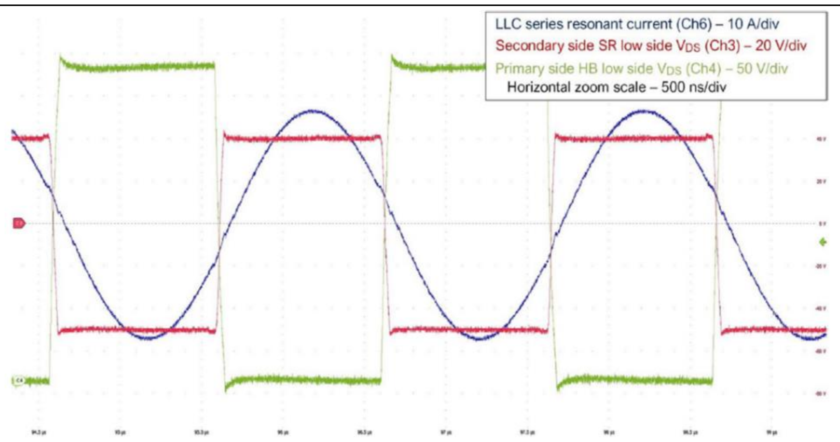

Figure 20 HB LLC waveforms during steady-state operation at 100% of the rated load

2.2 Triangular current mode (TCM) totem pole PFC

The increasing requirement of high efficiency in AC-DC SMPS application in the last decade has generated a significant interest in bridgeless topologies for the PFC stage, especially totem pole (TP) PFC, which can push the PFC efficiency above 99%. The benefits of the GaN-based hard-switching Continuous Conduction Mode (CCM) TP PFC are demonstrated in [9].

GaN has the unique benefit of zero-reverse recovery, which makes it an enabling technology for totem pole PFC, because the switch works as the main PFC switch in one half of the line cycle and then as a synchronous switch in the following half-line cycle. The body diode of, for example, a silicon superjunction device (such as CoolMOS™) is not suitable for such an operation due to its large reverse recovery charge.

Another important general benefit of this topology is the saved diode-bridge loss, which has a significant share of the total losses, for example, in the classic CCM boost PFC case.

If the switching frequency is limited to around or below 100 kHz, by using GaN it is possible to achieve peak efficiency exceeding 99% in the CCM TP PFC stage of a 3 kW SMPS design. This is needed to fulfil the most recent requirements of PSU peak efficiency ≥97.5%, especially in server and telecom applications.

Although the high efficiency and its relatively simple control make this topology very attractive, the system-level benefit is limited, because the switching frequency is still similar to that of silicon-based PFCs.

Even by using GaN, the significantly large turn-on losses are actually the bottleneck to pursue high frequencies combined with a reasonable efficiency target.

Compared with hard switching control implemented in the CCM TP PFC, a Triangular Current Mode (TCM) totem pole PFC topology promises additional benefits due to the device ZVS turn-on. As a potential enabler of higher switching frequency operation, this reduces the converter size while keeping similar efficiency levels as in the CCM version.

A big challenge introduced by the TCM operation is the large input current ripple which would require a large EMI filter and reduce the converter’s power density. Therefore, using an approach of interleaving 2 or 3 phases of the TCM PFC becomes the only option. Interleaving also brings advantages such as input current ripple cancellation, input EMI filter size reduction, and output capacitor current ripple cancellation.

The principle schematic of a 2-phase interleaved TCM totem pole PFC is shown in Figure 21. M1–M4 are the switches of the high-frequency leg, while S1-S2 are the low-frequency switching devices (active AC-line rectification).

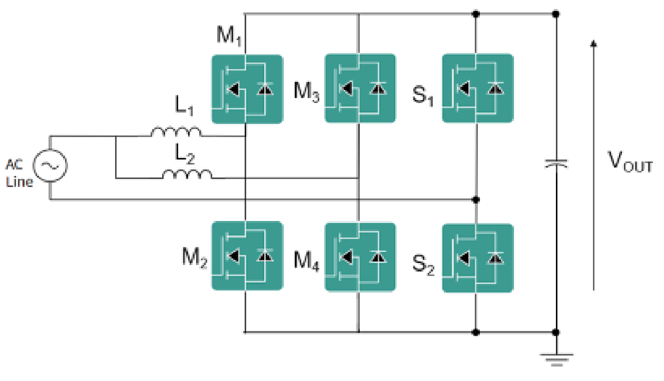

Figure 21 Principle schematic of a 2-phase interleaved TCM totem pole PFC

2.2.1 Value proposition of GaN in TCM totem pole PFC

To understand the benefits of GaN in TCM TP PFC, we have to dig a little more into the principle operation of the topology. The TCM totem pole PFC operates by dynamically switching the high-frequency leg to create a triangular-shaped inductor current waveform. This waveform, rather than the continuous current seen in CCM PFCs, enables ZVS turn-on, thus high efficiency. A dedicated control ensures that the inductor current passes through zero at the appropriate times to facilitate ZVS. Figure 22 shows the principle operation of each of the two phases interleaved in the schematics in Figure 21.

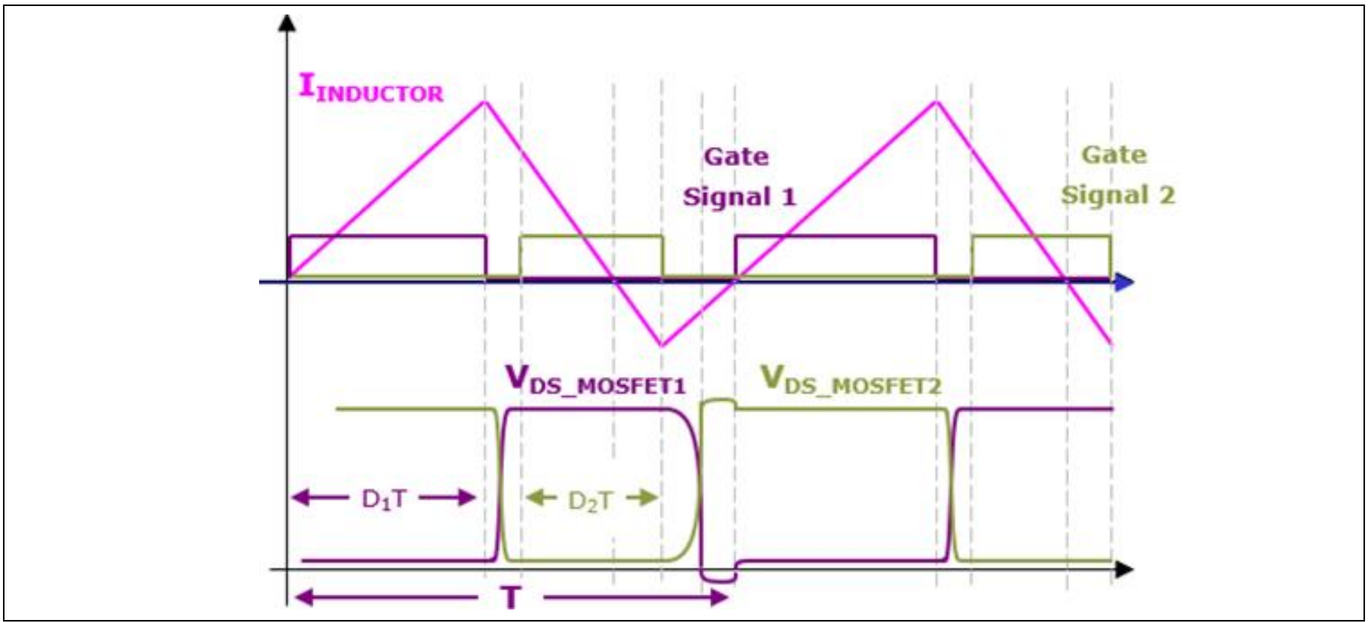

Figure 22 Principle operation of a Triangular Current Mode (TCM) totem pole PFC

It is clear then that the devices' switching frequency cannot be fixed, like in the CCM PWM modulation scheme, since frequency and dead-times must be adapted with the goal to achieve the ZVS turn-on. The negative current through the inductor is actually needed for discharging the output capacitance of the devices in the high frequency leg, thus achieving the ZVS. Therefore, a key figure-of-merit of the most suitable device for a TCM TP PFC is, once again, the $R_{DS(on)} \times Q_{oss}$ and the considerations already made for the LLC converter in Section 2.1.1 of this document (see Figure 4) are also valid here. In other words, GaN enables a high maximum switching frequency, with obvious benefits on the size of the PFC chokes as a consequence, and thus on power density. Another relevant benefit is provided by GaN's excellent FOM $R_{DS(on)} \times Q_g$ already discussed in Section 2.1.1; this also significantly contributes to the reduction of the needed dead-time.

Apart from the obvious combined positive impact on efficiency and power density, the reduction of the dead-time allowed by GaN devices, also potentially helps to reduce the input current Total Harmonic Distortion (iTHD), one of the general drawbacks of the TCM TP PFC topology. The reason behind this is the fact that the dead-times include the most "non-linear" portions of the switching waveforms. Benefits on EMI and simplification of EMI filtering are also to be expected. In general, special control techniques can help to maximize the performances benefit of this topology while minimizing the typical drawbacks of it.

State-of-the-art modulation schemes of TCM PFCs typically achieve ZVS over the whole range of input voltages and at any load condition by using a constant negative current in the positive half-wave. This requires the use of a zero-current-crossing detection-circuit and results in a widely varying switching frequency. The latter adversely impacts the size of the EMI filter which must effectively filter a wide frequency range. An alternative option is to operate the TCM modulation at a fixed switching frequency, but with a relatively large ripple current such that ZVS is achieved over the whole operation range. This system design, with a large current ripple that ensures ZVS for all input voltages, is typically dimensioned for the worst-case operating point at 90 V_{rms}. However, this results in a ripple current that is too large for high-line operation (e.g., at V_{in} = 230 V_{rms}) negatively affecting the efficiency at those conditions. The following application example shows an interesting hybrid fixed/variable frequency TCM modulation, which achieves high efficiency even at light-load conditions and a high input voltage, thus enabling ZVS even in MHz operations of GaN in PFC Stages.

2.2.2 Application example

In fixed frequency modulation of a PFC stage, e.g., a 2-phase interleaved totem pole as shown in Figure 21, ZVS can be naturally achieved with a relatively small inductance over the whole line cycle at the lowest input voltage of 90 V_{rms} and full power, since the inductor current reverses its direction in every switching cycle. When the same design, however, operates at a higher input voltage, e.g., at 230 V_{rms}, it still achieves ZVS but at a larger than necessary current ripple. This also applies for a part-load operation, where the average inductor current decreases but the ripple current stays unchanged compared to a full-load operation. This excessive current ripple increases the rms value of the inductor current, which affects the winding losses of the inductor as well as the conduction losses of the switches. Furthermore, the current ripple also directly influences the magnetization of the inductors and thus also the core losses.

Therefore, reducing the ripple current while still operating in ZVS offers the possibility to further reduce the system losses. A good option to achieve a reduction of an unnecessarily high current ripple is the control method of the hybrid fixed/variable frequency TCM modulation which increases the switching frequency whenever the current ripple is larger than what is desired to achieve full ZVS. This control technique is shown in the present application example and described in Figure 23.

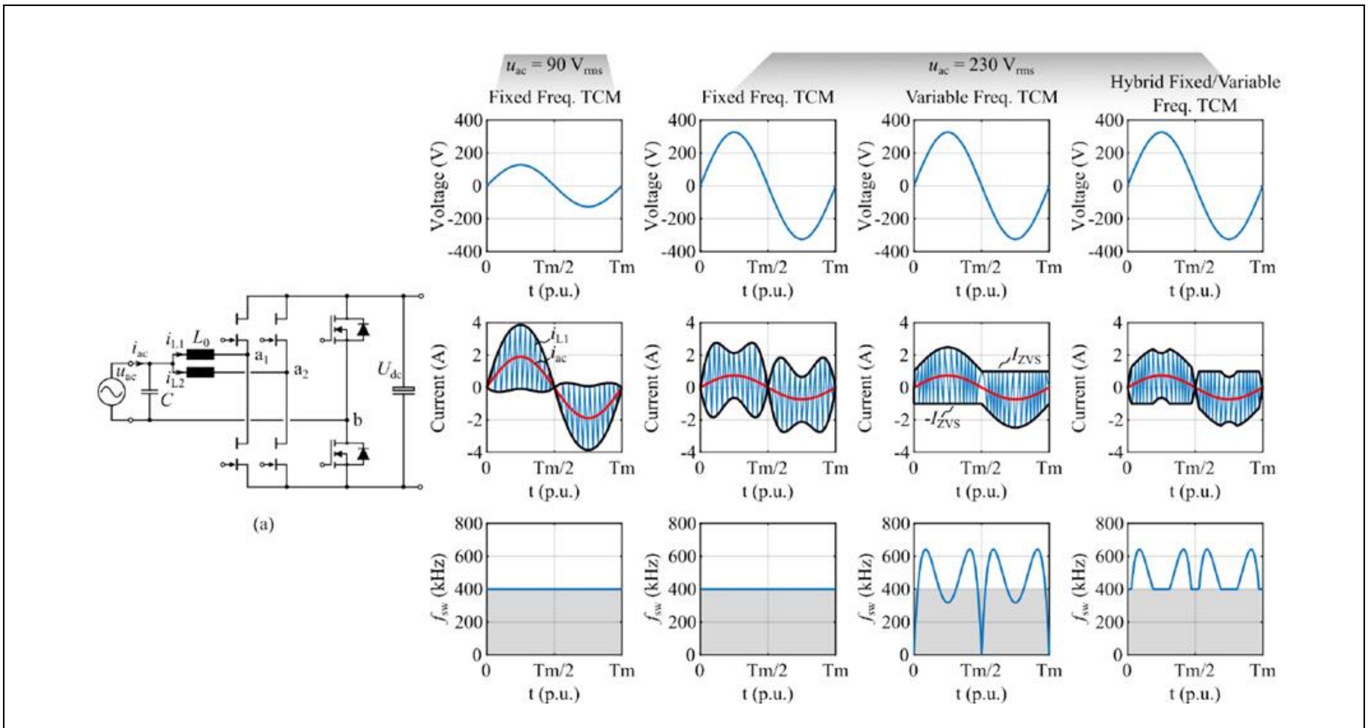

Figure 23 Principle schematics and operation of a 2-phase interleaved TCM TP PFC with hybrid frequency modulation

As explained in detail in [10], the proposed modulation method has been implemented and verified on the PFC stage of two different systems. The first one is a passively cooled 240 W dual-port USB-C charger with a power density of 42 W/inch³ (2.6 kW/L) where the hybrid modulation is applied to the totem pole PFC. In the second system the proposed modulation scheme is applied to a triple-interleaved 220 W classic boost PFC with an active bridge rectifier in a forced air-cooled system with a power density of 138 W/inch^3 (8.4 kW/L).

The main goal of the modulation concept presented in this application example is to exploit the excellent soft-switching behavior of the GaN devices; this allows to dynamically increase the switching frequency of any PFC stage depending on the operating point. This reduces the current ripple of the inductor current while still maintaining ZVS, thus achieving a total saving of around 20% of the system losses, depending on the operating point. The implementation effort of this novel control concept is very low, since only a new target switching frequency needs to be calculated without the need for additional hardware or measurement circuitry. For instance, no dedicated zero-current-crossing detection-circuit is needed.

Moreover, a detailed loss analysis shows that the reduction in the system losses comes mainly from the reduction of the core losses. This is a consequence of the smaller peak-to-peak deviations of the magnetic flux that arises from smaller ripples of the inductor current. Additionally, a reduced rms current of the inductor also leads to savings of the winding losses.

2.3 Cyclo-converter

With the trends of increasing PV panel power and multi-PV panel microinverter products, GaN can offer system benefits such as:

- Higher efficiency, reduced losses, and heat dissipation, allowing for higher power and more integration
- Higher switching frequency allows reducing system costs by reducing size

The single-phase cycloconverter-type microinverter (Figure 24) is one case of a resonant converter with a single stage and fewer power switches. It has the benefit of efficient high frequency operation due to ZVS. This results in a higher power density and a smaller size, and its modulation scheme allows a large soft-switching range, and bidirectional power transmission ability, which is superior to other microinverter topologies.

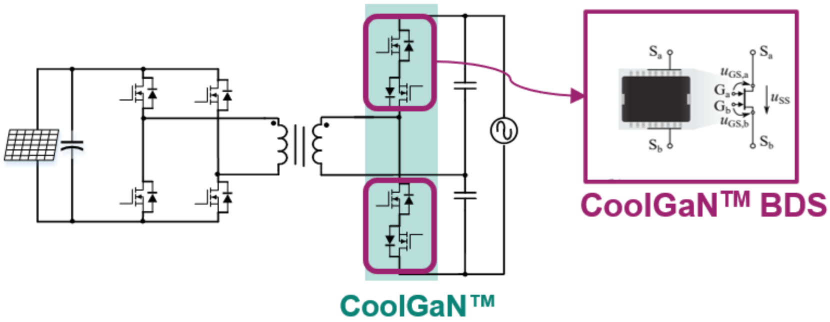

Figure 24 Cycloconverter microinverter basic topology

2.3.1 Value proposition of GaN in a cyclo-converter

GaN has low Q_{oss} to enables fast and easy soft switching at a high switching frequency. Table 1 shows a Q_{oss} FOM comparison between GaN and Si, showing that GaN can have as low as 9% Q_{oss} of the same $R_{DS(on)}$ Si FET.

Table 1 Q_{oss} FOM comparison between Gan and Si

	$V_{(BR)DSS}$ [V]	$R_{DS(on)} \times Q_{oss}$ [mΩ × µC]
CoolMOS™	600	100%
CoolGaN™	650	9%

Low Q_{oss} means faster drain-source transition to reach ZVS in a shorter dead-time, this becomes critical especially when the resonant inductor current is small near the zero crossing of the AC line voltage as shown in the simulation in Figure 25.

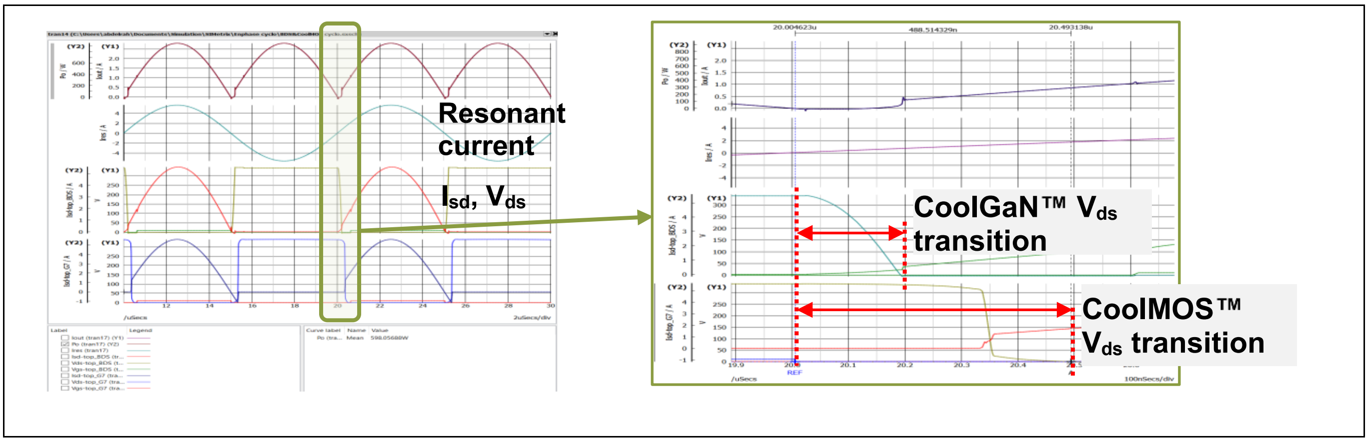

Figure 25 Comparison of drain-source transition of Gan vs. Si (left), zoomed-in V_{ds} transition (right)

GaN has the lowest Q_{gd} and total Q_g, to enable the fastest switching time and lowest switching loss. Figure 26 shows a gate charge profile comparison of GaN vs. Si vs. SiC. Although cycloconverters are normally soft switched, switching speeds and losses are still important in this topology, because in some operations, the phase-shift between primary and secondary bridges is used to modulate power. This leads to non-zero current switching and turn-off switching loss, which reduces efficiency especially at higher switching frequency.

Figure 27 shows the simulation of an example of operation with primary-secondary phase shift causing the resonant current to be switched at non-zero current.

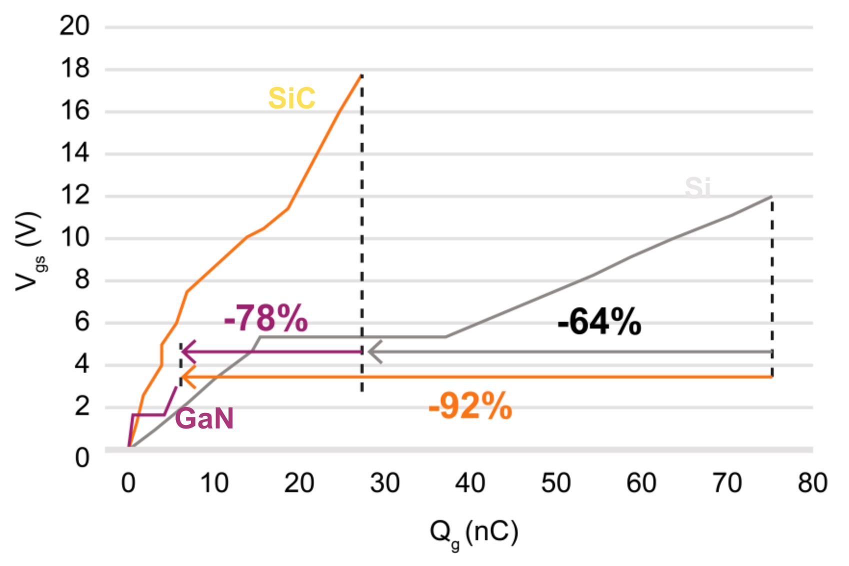

Figure 26 Gate charge profile comparison of GaN vs. Si vs. SiC

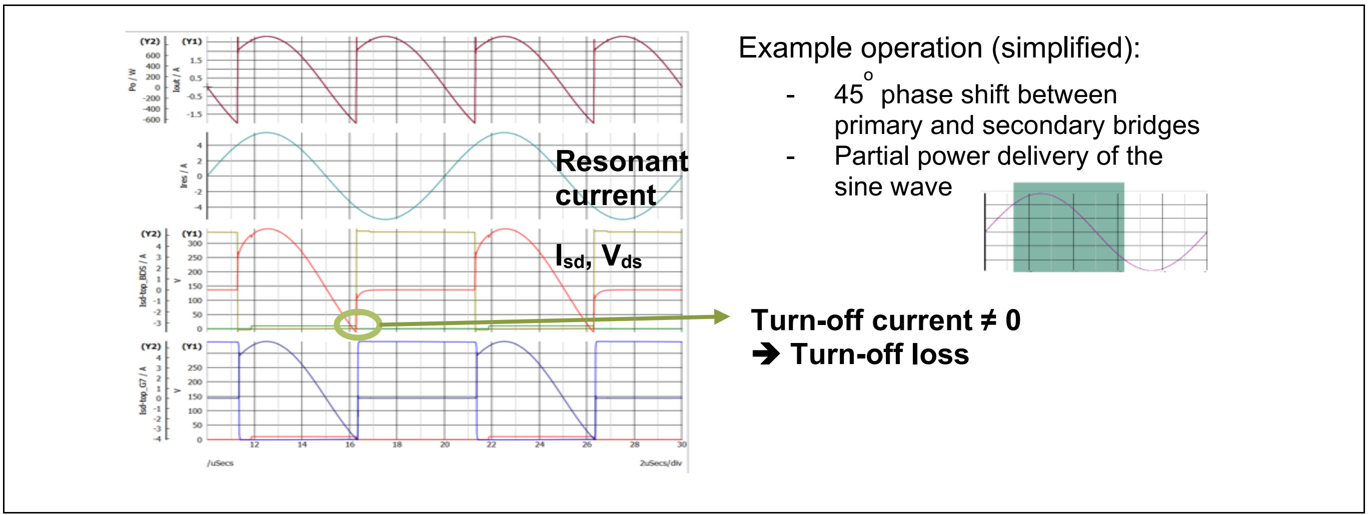

Figure 27 Example of a cyclo-converter operation with non-zero current switching and turn-off switching losses

Another differentiation aspect of GaN compared to Si and SiC is that it is a lateral device, while Si and SiC are vertical structures. While this enables monolithic integration in GaN devices, such as a true normally-off monolithic bidirectional switch, which can replace the two back-to-back switches of the cyclo-converter as shown in Figure 28. This offers a cost-effective high-performance solution, smaller PCB area, and BOM reduction.

The monolithic bidirectional GaN has the most effective die size utilization compared to two back-to-back switches. Figure 28 shows a chip area comparison of 2x unidirectional GaN switches vs. 1x monolithic bidirectional GaN switch for the same $R_{DS(on)}$, it shows the benefit of $R_{DS(on)}/mm^2$ and consequently the improved switching losses and system cost.

Furthermore, GaN's lateral structure enables integration of more circuit elements, such as gate drivers, protection features and control blocks, to provide an unbeatable BOM reduction and ease of use.

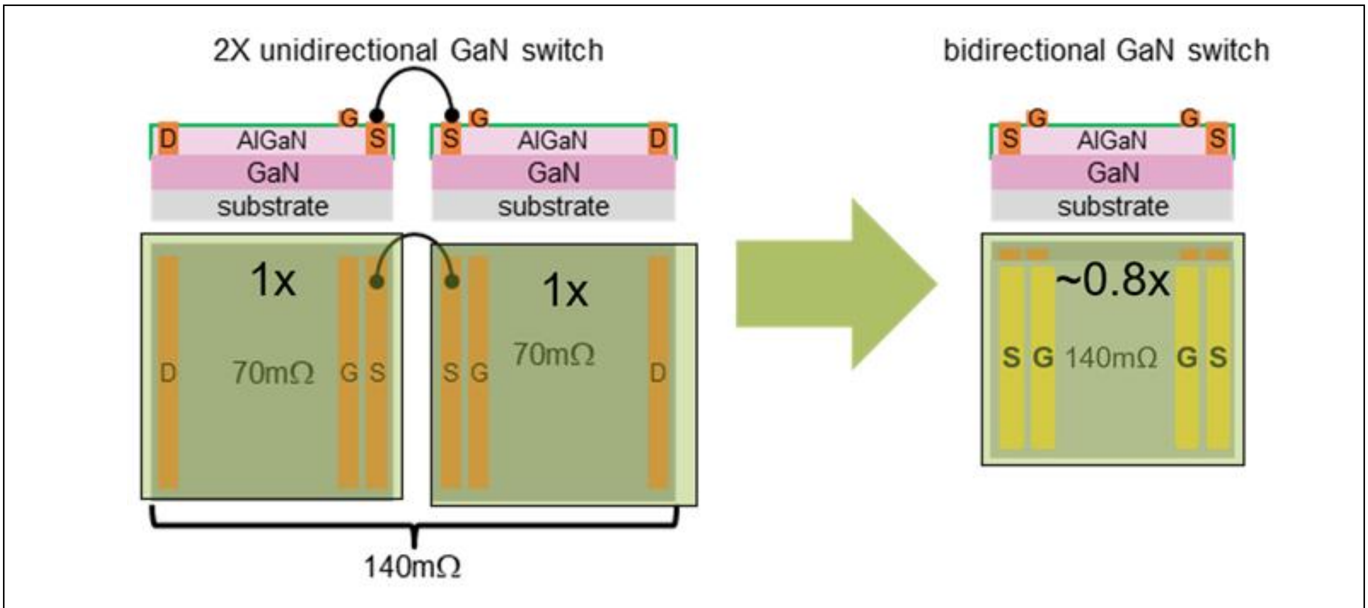

Figure 28 Chip area comparison of 2x unidirectional GaN switches vs. 1x monolithic bidirectional GaN switch

2.3.2 Application example

The above-mentioned benefits of GaN semiconductors, in particular, monolithic bidirectional GaN switches, can also be leveraged in three-phase cycloconverters. Three-phase cycloconverters offer the advantage of reduced system volume by merging the PFC stage and the DC-DC stage of classic two-stage systems into a single converter stage. This is especially interesting for space-constraint applications, such as onboard chargers (OBCs) in electric vehicles.

The requirements for OBCs are challenging, because they have to be able to operate at balanced and unbalanced three-phase grids as well as single-phase grids to ensure worldwide compatibility. OBCs also have to support bidirectional power flow to enable vehicle-to-X operation. At the same time, minimum efficiency targets as well as volumetric targets have to be met.

A very promising topology candidate for OBCs is the X-rectifier topology [11] as shown in Figure 29 which features asymmetric power flow capabilities in all phases as well as the ability to handle phase voltage unbalances. This topology utilizes M-BDS GaN devices in a half-bridge configuration for each grid phase on the primary side and unidirectional GaN devices on the secondary. The M-BDS GaN switches only have to block the phase-to-neutral voltage instead of the phase-to-phase voltage as with typical three-phase converters. The benefits of this all-GaN solution are the reduced output charges of the GaN devices which allows achieving soft-switching with minimum currents. Since this converter is operated with a DAB modulation scheme, high currents must be turned off occasionally (as described in detail in Section 2.5). This can be done most efficiently with GaN devices with low gate charges which lead to the lowest turn-off losses among all semiconductor technologies.

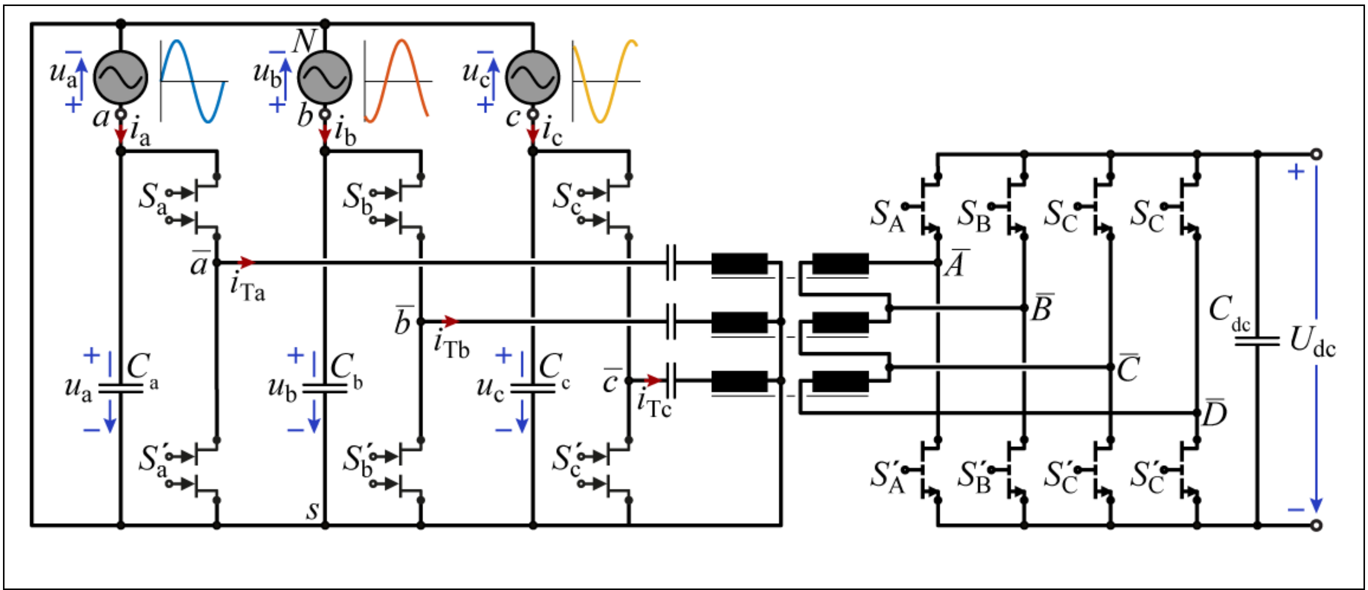

Figure 29 Schematic of X-rectifier cycloconverter topology

2.4 Hybrid flyback

The hybrid flyback is well known as the asymmetrical half-bridge flyback, shown in Figure 30. It is an isolated DC-DC power topology suitable for mid-power applications where a flexible input-to-output voltage is required, for example, USB-PD adaptors, battery chargers, and lighting. With proper control methods and dimensioning, it can achieve both ZVS and ZCS, and therefore high efficiency. With such soft-switching characteristics, the hybrid flyback is suitable for high frequency operation that helps reduce the size of the magnetic components. The term "hybrid" used for this topology is due to the energy processed in the transformer. A portion is transferred in forward-mode from the primary to secondary side across the transformer but another portion is stored in the magnetic core of the transformer before it is sent to the secondary side. This portion depends on the input voltage, output voltage, and the dimensioning of the converter.

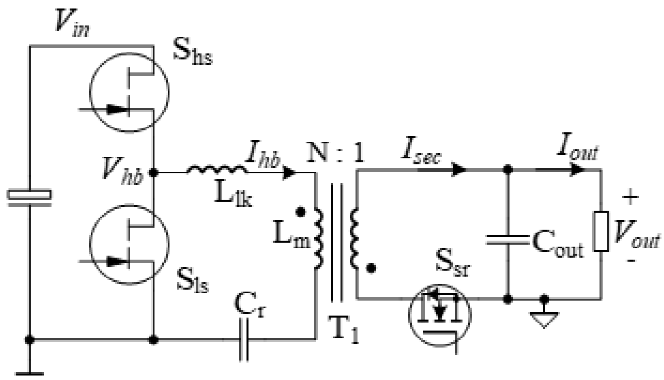

Figure 30 Hybrid flyback topology

Careful dimensioning the hybrid flyback can achieve ZVS. When operated in resonance with the LC tank formed by the transformer leakage inductance and the capacitor in series with the transformer, ZCS can be achieved. ZCS in the secondary ensures low noise and undesired oscillations, and hence, improved efficiency.

Figure 31 shows the waveforms of the hybrid flyback in resonant operation. Dead-times are provided between the on time of the HS and LS allowing ZVS. ZCS is achieved in the secondary side when operated in resonance as explained before.

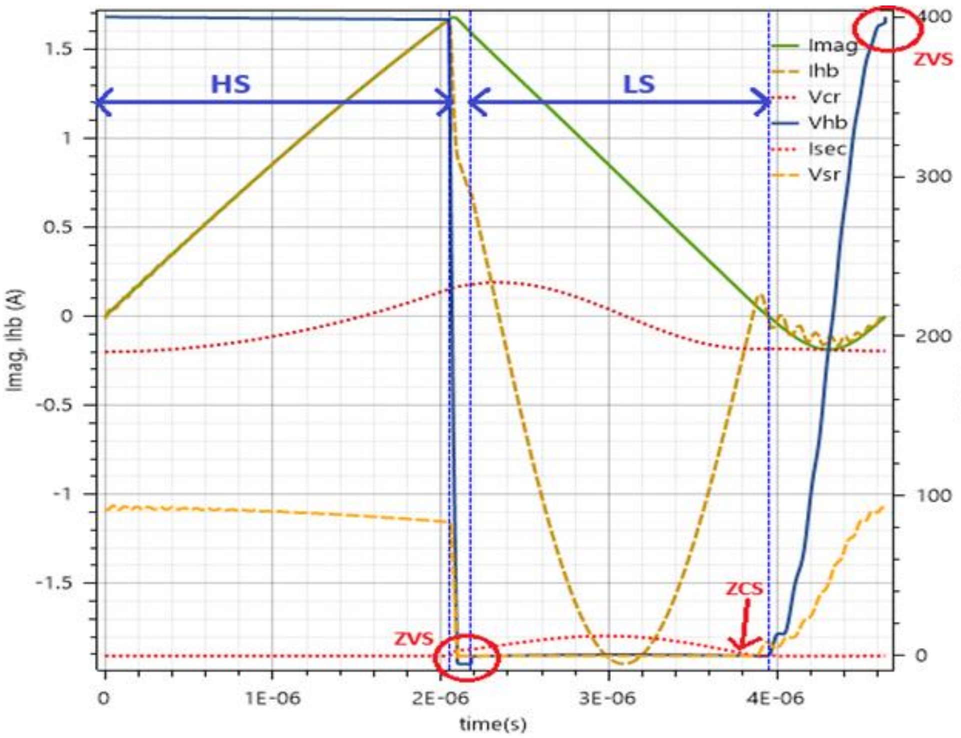

Figure 31 Hybrid flyback topology waveforms

2.4.1 Value proposition of GaN in hybrid flyback

Many applications aim for a small size and efficient operation to guarantee good thermal behavior. To achieve those targets, high switching frequency is desired because it can help reduce the size of the magnetic components which are one of the major contributors for the size of the power supply. Additionally, EMI filter components could be reduced when higher switching frequencies are used.

The parasitic capacitance of the power switches (C_{oss}) is one of the major limitations for high frequency operation. They not only impact the dead-times, thus limiting the duty cycle used to transfer energy to the secondary side, but they also influence the amount of energy required just to ensure ZVS.

GaN devices, compared to other technologies like silicon, offer the best FOM of $R_{DS(on)} \times C_{oss}$, that makes them the most suitable devices to operate the converter at the desired high switching frequency.

2.4.2 Application example

Mid-power applications (75 W–500 W) such as portable power supplies requiring high power density, low weight, and a wide input and output voltage range are most suitable for this topology. Examples are USB-PD adaptors (as in Figure 32), eBikes and power tool chargers, battery chargers in general, and lighting applications.

When very flat designs are required, the hybrid flyback is a great option due to the fact that it does not need an additional series inductor compared to an LLC and therefore benefits the most from PCB winding transformers.

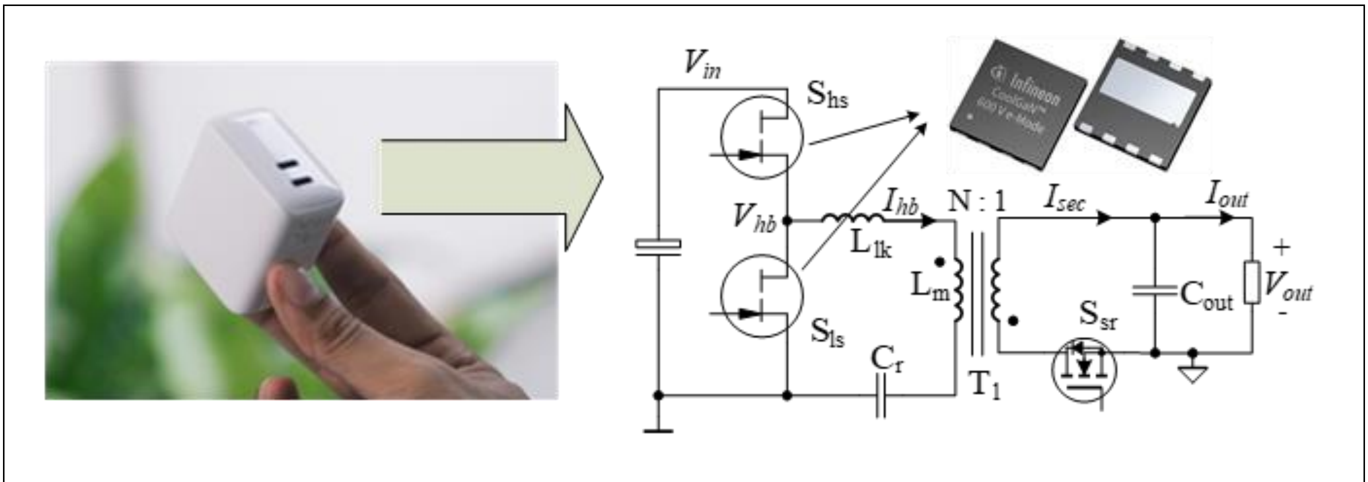

Figure 32 Hybrid flyback USB-PD application example using CoolGaN™ devices

2.5 Dual Active Bridge (DAB)

The dual active bridge (DAB), shown in Figure 33, is a widely used topology in power electronics, particularly in high-power applications, such as renewable energy systems, electric vehicles, and data centers. This topology has gained significant attention in recent years due to its ability to efficiently transfer power between two DC voltage sources, while also providing galvanic isolation and bidirectional power flow capabilities. The DAB converter consists of two full-bridge converters, one on the primary side and one on the secondary side, which are connected through a high-frequency transformer. By using a phase-shift modulation technique, the DAB converter can simultaneously achieve high efficiency and high-power density. High efficiency can be achieved because of DAB's ability to achieve soft-switching in all four bridge legs.

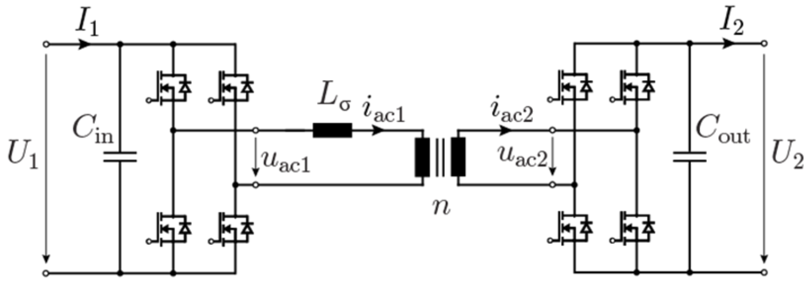

Figure 33 Dual Active Bridge (DAB) topology

The main fundamental difference of the DAB from the LLC is that the DAB is not a resonant topology, whereas the LLC is. In the LLC, there is a resonant tank that limits the power transfer between the primary and the secondary side, but in the DAB there is solely an inductor. Note that another fundamental difference is that the DAB is inherently bidirectional, whereas the LLC by itself is unidirectional, but can be made bidirectional by splitting the resonant tank on both sides, to convert it into a CLLC.

Finally, there is also a difference in the modulation. Typically, the LLC operates with all bridge legs featuring a 50% duty cycle, and the only degree of freedom that is used is the switching frequency (f_{sw}). In a DAB, there are up to 4 degrees of freedom: the duty cycle of the primary side (D1), the duty cycle of the secondary side (D2), the phase shift between the primary side and the secondary side (φ), and the switching frequency (f_{sw}).

As a result, the DAB offers more degrees of freedom to control, which also enables, compared to an LLC, a suitable way to address applications which require a wide input and wide output voltage range. This is a very nice feature, for instance, for battery chargers (be it industrial or automotive), since the DC-DC converters in these applications typically required a wide voltage transfer ratio. However, when optimizing a DAB for wide voltage ranges, it can be done with several objectives. For instance, it can be optimized for reduced RMS currents, and hence lowest conduction losses [12], or it can be optimized for soft-switching [13]. In [12], the switches of the secondary side were low-voltage switches, so they are not so critical if they enter a hard-switching regime. But, for instance, in onboard or off-board EV chargers, the secondary side devices are high-voltage devices, which suffer substantially more from hard-switching losses. Therefore, optimizing for soft-switching for a wide output voltage range is possible with a DAB.

2.5.1 Value proposition of GaN in the DAB topology

The main value propositions of GaN in a DAB are:

- GaN is highly suitable for high-frequency soft-switching applications, with low Q_{oss}, linear C_{oss}, and very low soft-switching (turn-off) losses
- It can also go into hard-switching operating modes if needed, e.g., if the battery voltage is very discharged

This latter case can also be enabled by SiC, but on the other hand, cannot be fulfilled by silicon superjunction technologies. Therefore, with high-switching frequency enablement with GaN, not only can the DAB be built in a very efficient way for a wide voltage range operation, but it can also be done in a very compact manner, increasing power density.

2.5.2 Application example

A great application example for the DAB and its use is a 10 kW onboard charger (OBC) that Infineon built together with ETH Zürich [13], which is seen in Figure 34. This is an ultraflat profile charger, featuring Infineon's CoolGaN™ devices for all the active switches, as well as CoolSiC™ diodes.

This OBC has several key features. Firstly, its ultraflat profile is an outcome of the high switching frequency that is used in the converter. The Vienna rectifier switches at 560 kHz, enabling very small boost inductors, and the DABs have a switching frequency that varies between 180 kHz and 330 kHz. Typically, DABs are modulated with a fixed switching frequency, but to enable ZVS over a wider operating output voltage range in this converter, the switching frequency is made variable [13]. Therefore, with the switching frequency of the DAB starting at 180 kHz, it enables a flat realization of the transformers. Secondly, the DABs feature a very wide output voltage range, i.e., from 200 V to 1000 V – enabled also by either the series or parallel configuration of the DABs, as the output of each DAB is 100 V to 500 V. And finally, the converter utilizes the synergetic control of the PFC and DC-DC, using the 1/3 PWM modulation. This enables an efficiency boost of over 1% at half-load operation.

For more details on the converter and the DAB modulation, refer to the comprehensive publication by Y. Li et al. [13].

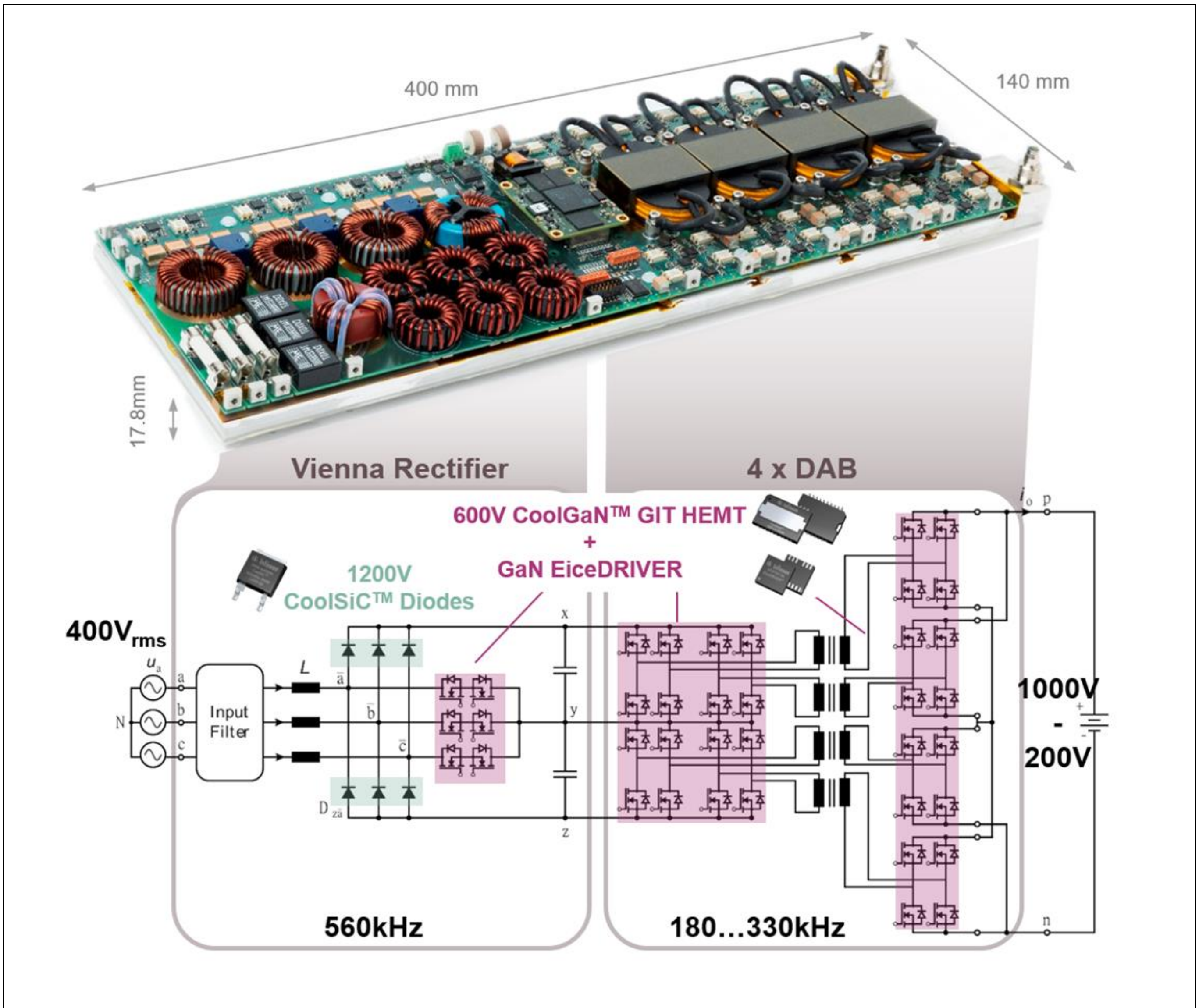

Figure 34 Ultraflat 10 kW onboard charger featuring CoolGaN™

3 Related resources

- GaN transistors (GaN HEMTs)
- E-mode and D-mode GaN power transistors: real-world performance compared to theory
- Gallium nitride - Reliability and qualification of CoolGaN™ GIT HEMTs
- Gate drive configurations for GaN power transistors
- 2500 W full-bridge totem-pole power factor correction using CoolGaN™
- An industry game-changer: 300 mm power GaN technology

References

[1] E. Persson and F. Di Domenico, Infineon Technologies AG: *Optimizing PCB layout for HV CoolGaN™ power transistors*, July 2023; Available online

[2] B. Zojer, F. Di Domenico and E. Persson, Infineon Technologies AG: *Operation and features of high-voltage CoolGaN™ Transistors*, October 2024; Available online

[3] B. Zojer, Infineon Technologies AG: *Gate drive configurations for GaN*, April 2024; Available online

[4] A. Nakajima: *Power loss limit in unipolar switching devices: Comparison between silicon superjunction devices and wide bandgap devices*, IEEE Trans. Electron Devices, vol. 56, no. 11, pp. 2652- 2656, 2009.

[5] M. Kasper, R. Burkart, and G. Deboy: *ZVS of Power MOSFETs Revisited*, IEEE Transactions on Power Electronics, vol. 31, no. 12, pp. 8063-8067, 2016.

[6] G. Deboy, O. Haeberlen, and M. Treu: *Perspective of loss mechanisms for Silicon and Wide bandgap Power devices*, CPSS Transactions on Power Electronics and Applications, vol. 2, no. 2, 2017.

[7] W. Zhang and S. Henning: *Impact of Planar Transformer Winding Capacitance on Si-based and GaN-based LLC Resonant Converter*, in Applied Power Electronics Conference (APEC), Long Beach, CA, 2013.

[8] Infineon Technologies AG: *3.3 kW high-frequency and high-density PSU for server and datacenter applications_REF_3K3W_HFHD_PSU*, January 2025; Available online

[9] S. Abdel-Rahman and E. Persson, Infineon Technologies AG: *CoolGaN™ totem-pole PFC design guide and power loss modeling*, 2019; Available online

[10] M. Kasper, J. Azurza Anderson, S. Weihe, and G. Deboy: *Hybrid Fixed/Variable Frequency TCM Average Current Control Method Enabling ZVS MHz Operation of GaN HEMTs in PFC Stages*, IEEE Transactions on Power Electronics, 2022.

[11] D. Zhang, S. Weihe, J. Huber, and J. W. Kolar: *Single-Stage Isolated Bidirectional Extended-Functionality X-Rectifier for EV Chargers with Three/Single-Phase AC Input Capability*, in ECCE US, 2024.

[12] F. Krismer and J. W. Kolar: *Efficiency-Optimized High-Current Dual Active*, IEEE Transactions on Industrial Electronics, vol. 59, no. 7, 2012.

[13] Y. Li, J. A. Anderson, M. Haider, J. Schäfer, J. Miniböck, J. Huber, G. Deboy, and J. W. Kolar: *Optimal Synergetic Operation and Experimental Evaluation of an Ultracompact GaN-Based Three-Phase 10-kW EV Charger*, IEEE Transactions on Transportation Electrification, vol. 10, no. 2, 2024.

[14] F. Krismer: *Modeling and Optimization of Bidirectional Dual Active Bridge DC-DC Converter Topologies*, PhD Thesis, ETH Zurich, 2010.

Revision history

Document revision	Date	Description of changes
V 1.0	2025-09-11	Initial release

Trademarks
All referenced product or service names and trademarks are the property of their respective owners.

Edition 2025-09-11

Published by

Infineon Technologies AG

81726 Munich, Germany

Do you have a question about this document?

Email: erratum@infineon.com

Document reference

AN152548